

H^-/H^0 INJECTION into PROTON DRIVERS by
LORENTZ LASER assisted STRIPPING

- $H^- \rightarrow H^0_{(1s)} \rightarrow H^0_{(n\beta)} \rightarrow p^+ + e^- !$

LO

- Angular dispersion of H^0 beam

Jason et al
IEEE NS-28 (1981) 2704

LA

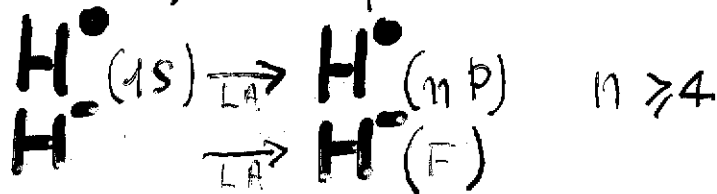
- Resonant V
 $\nu_L, \chi, \alpha, n, B$
- Staining tuned $\Delta\nu / \Delta p$
- Power density I_{FP}

LO

- Angular dispersion of p^+ beam
- | | |
|---------------|-----|
| Yamane '98 | '98 |
| Suzuki '99 | '99 |
| Druzhinin '99 | '99 |
| U.G. '00 | '00 |
| Yamane '01 | '01 |
| | |

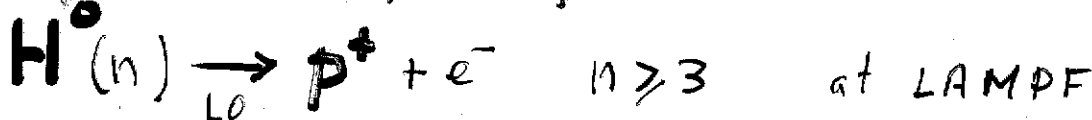
$$H^- \xrightarrow{LA} H^0_{(F)} \xrightarrow{LO} p^+ + 2e^- \text{ U.G. c.b. 9/V/02 ?}$$

- Results from experiments that used or measured

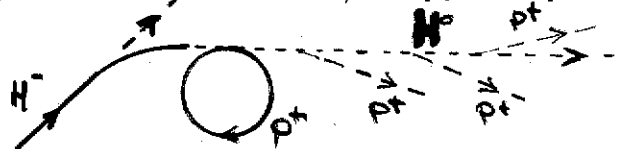


at LAMPF

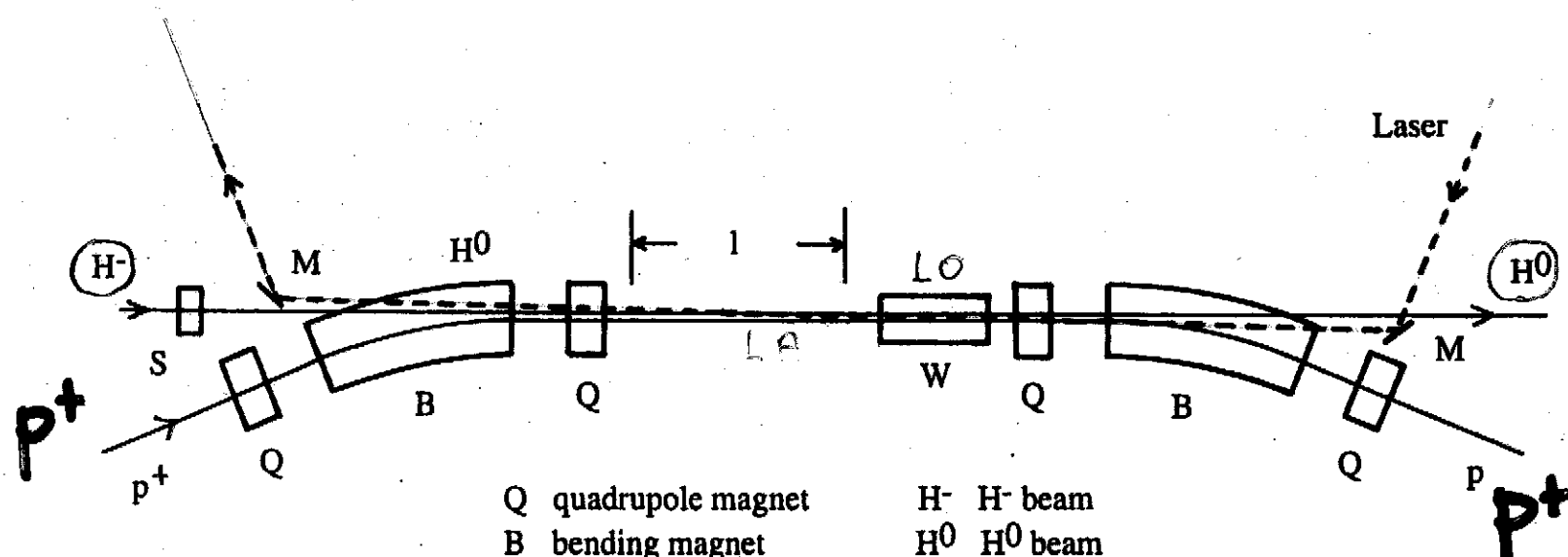
High power density Fabry-Pérot PVLAS at LNL (Legnaro)



- Integration-optimization: ($V_{FP}, \chi, \alpha, n, \Delta p / p, I_{FP}, B$)
- Comments, conclusions



I.Yamane PR ST A&B1(1998)
053501



Q quadrupole magnet

H^- H^- beam

B bending magnet

H^0 H^0 beam

S stripper magnet for H^-

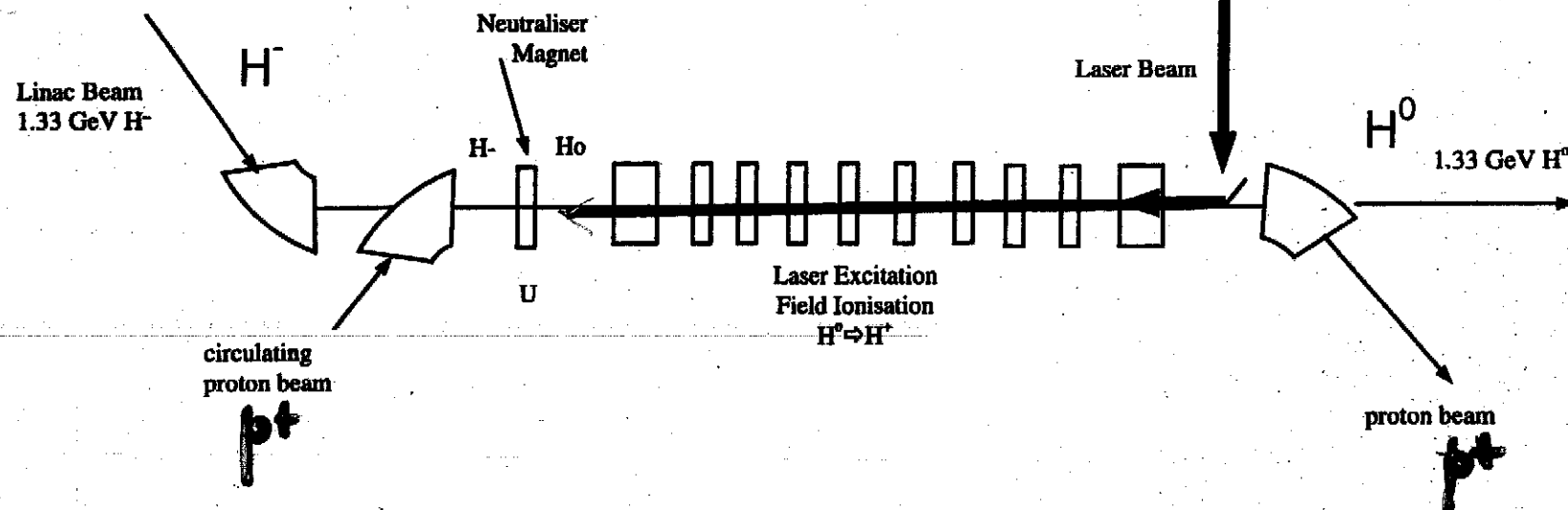
p proton beam

M laser mirror

I H^0 -Laser interaction region

W stripper for $H^0(3P)$ atoms

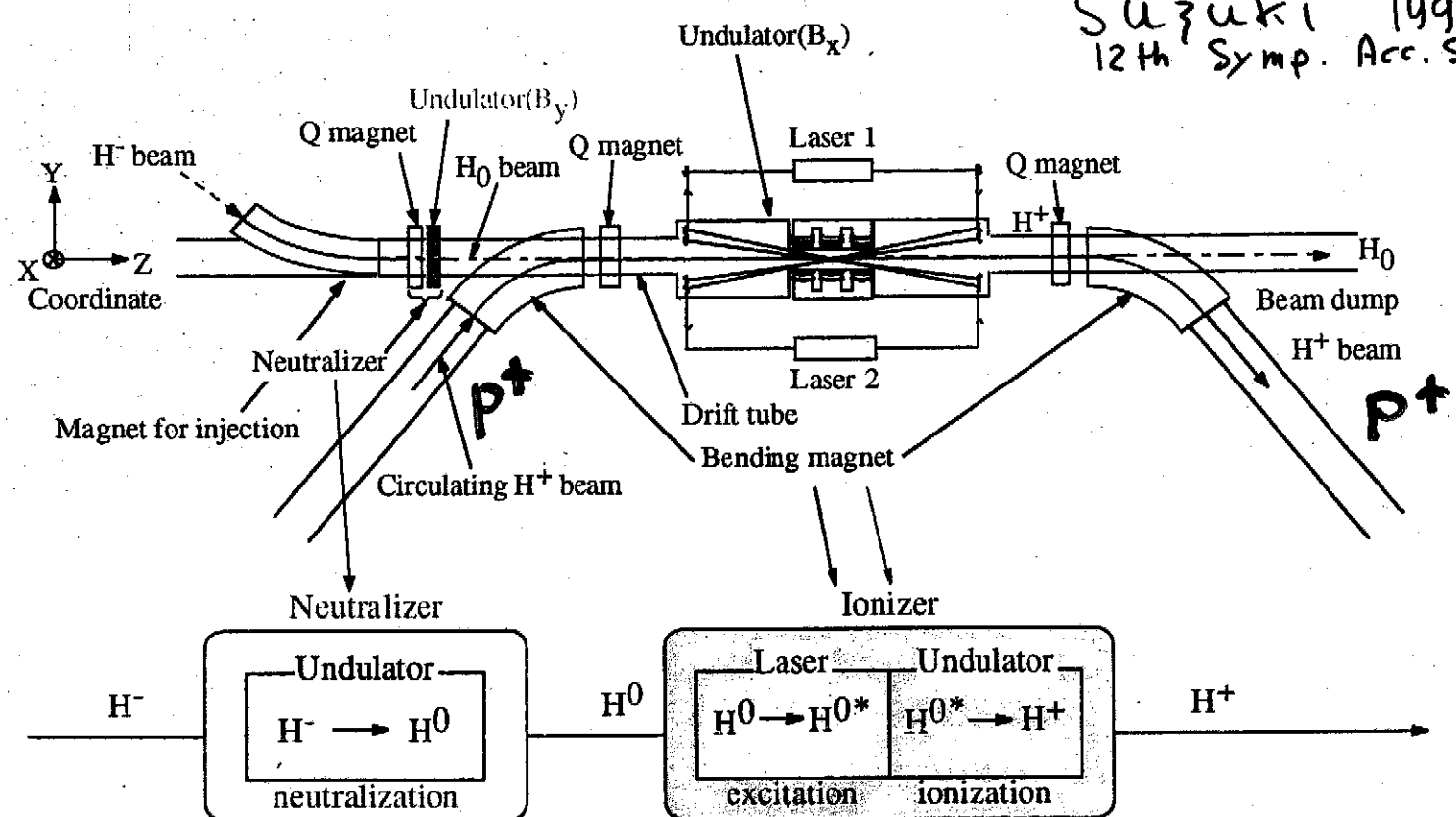
ESS Schematic



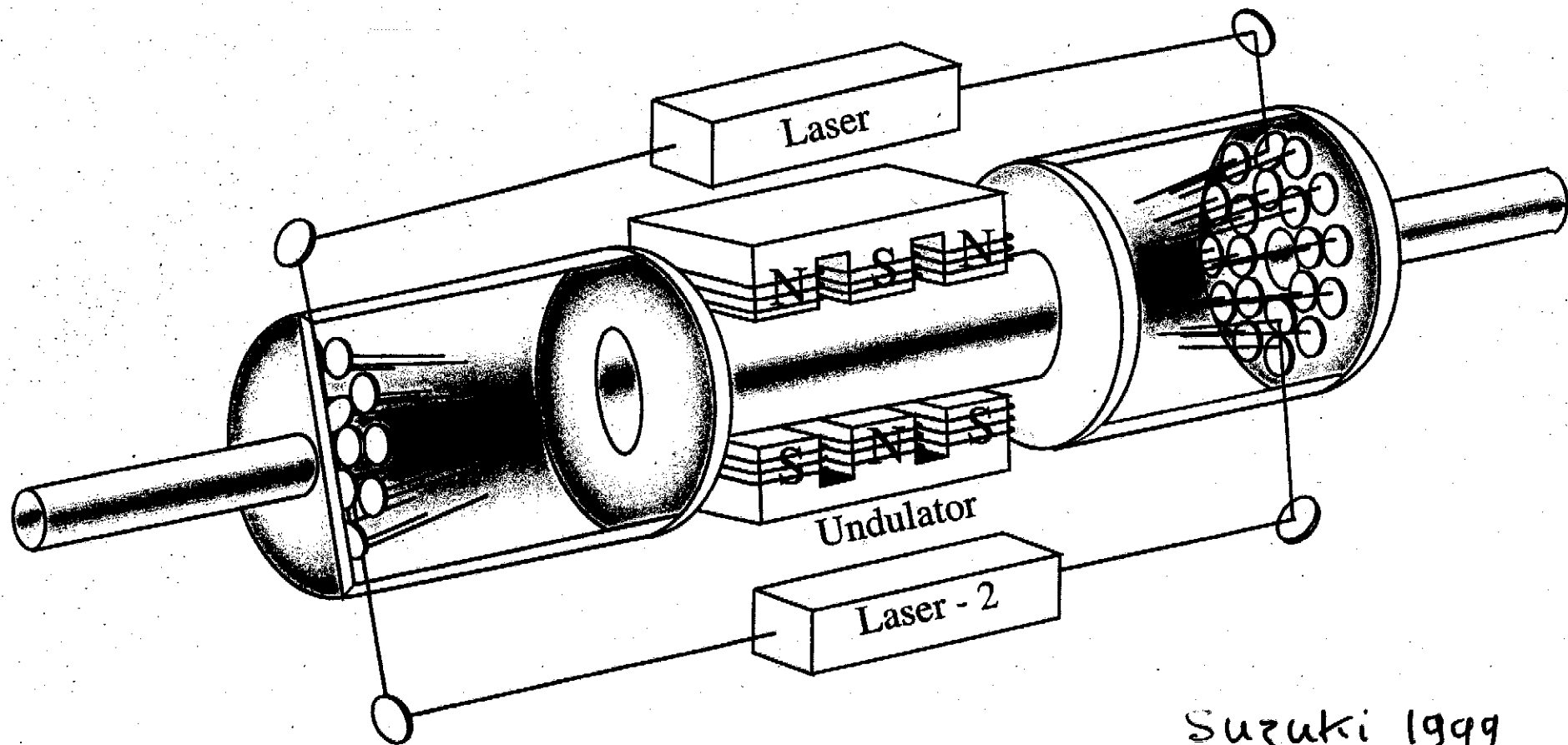
Accumulator
Ring

DoLUCE

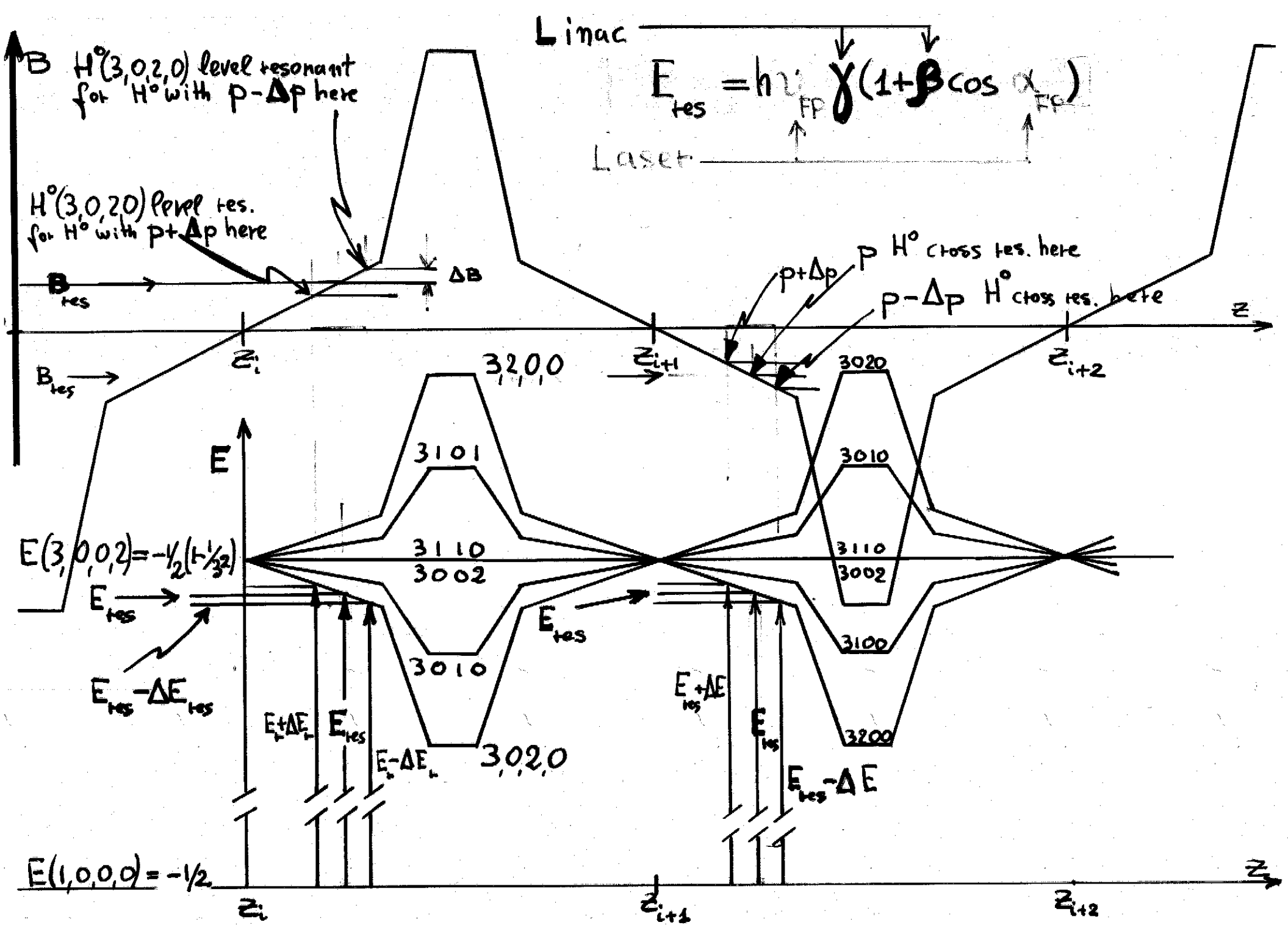
Double Lasers and Undulator Charge Exchange



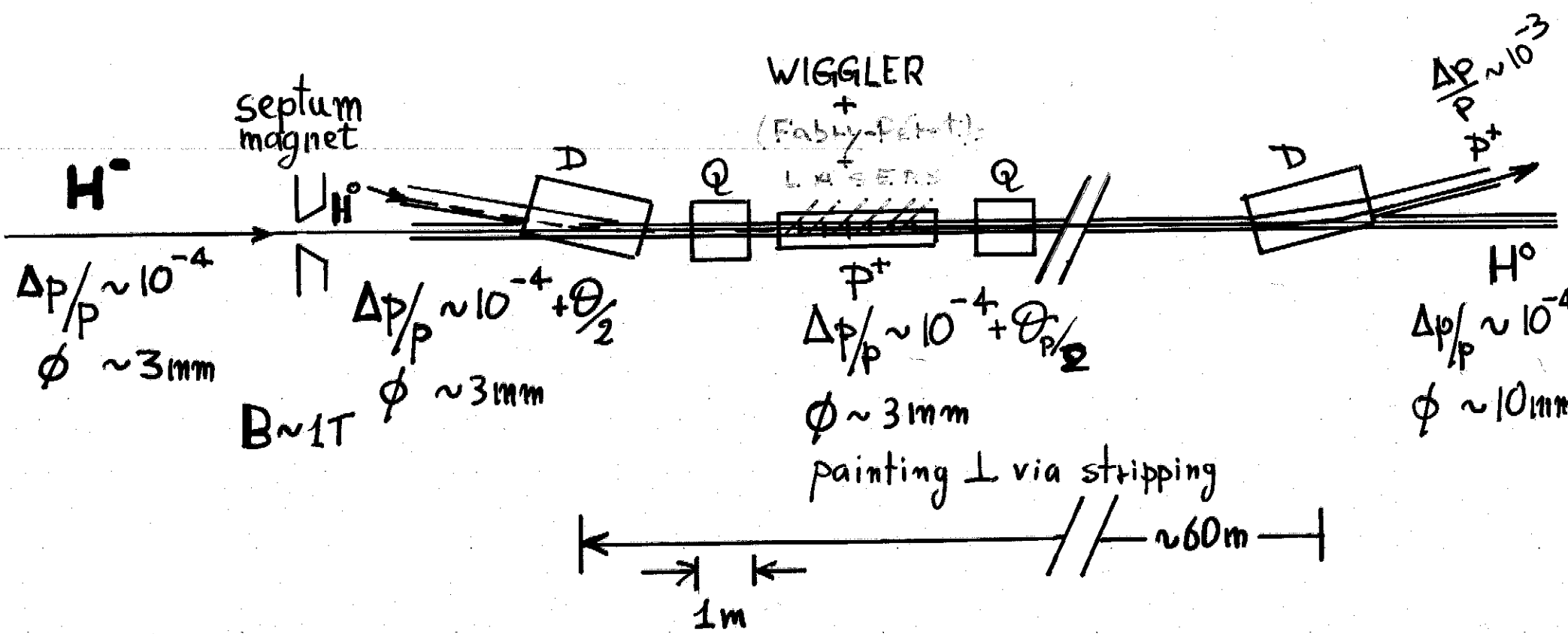
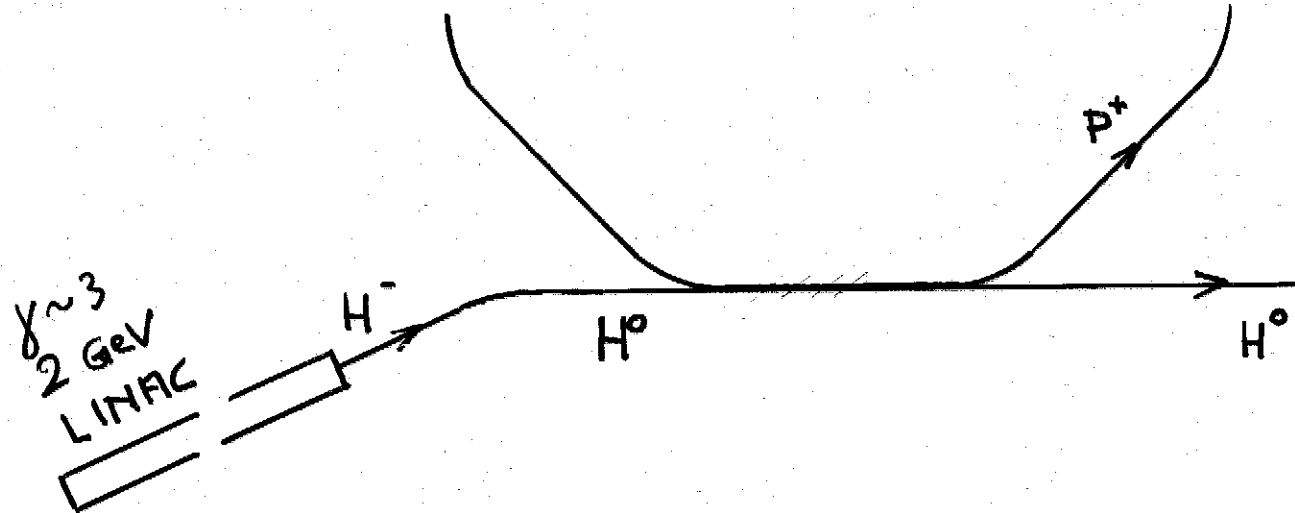
DoLUCE



Suzuki 1999



U.S. + M.P.
NIM #451(2000)318



Donahue et al. 1981

IEEE NS28 (1981) 1203

DOWNSTREAM
MAGNET

$E = 3 \beta y B$

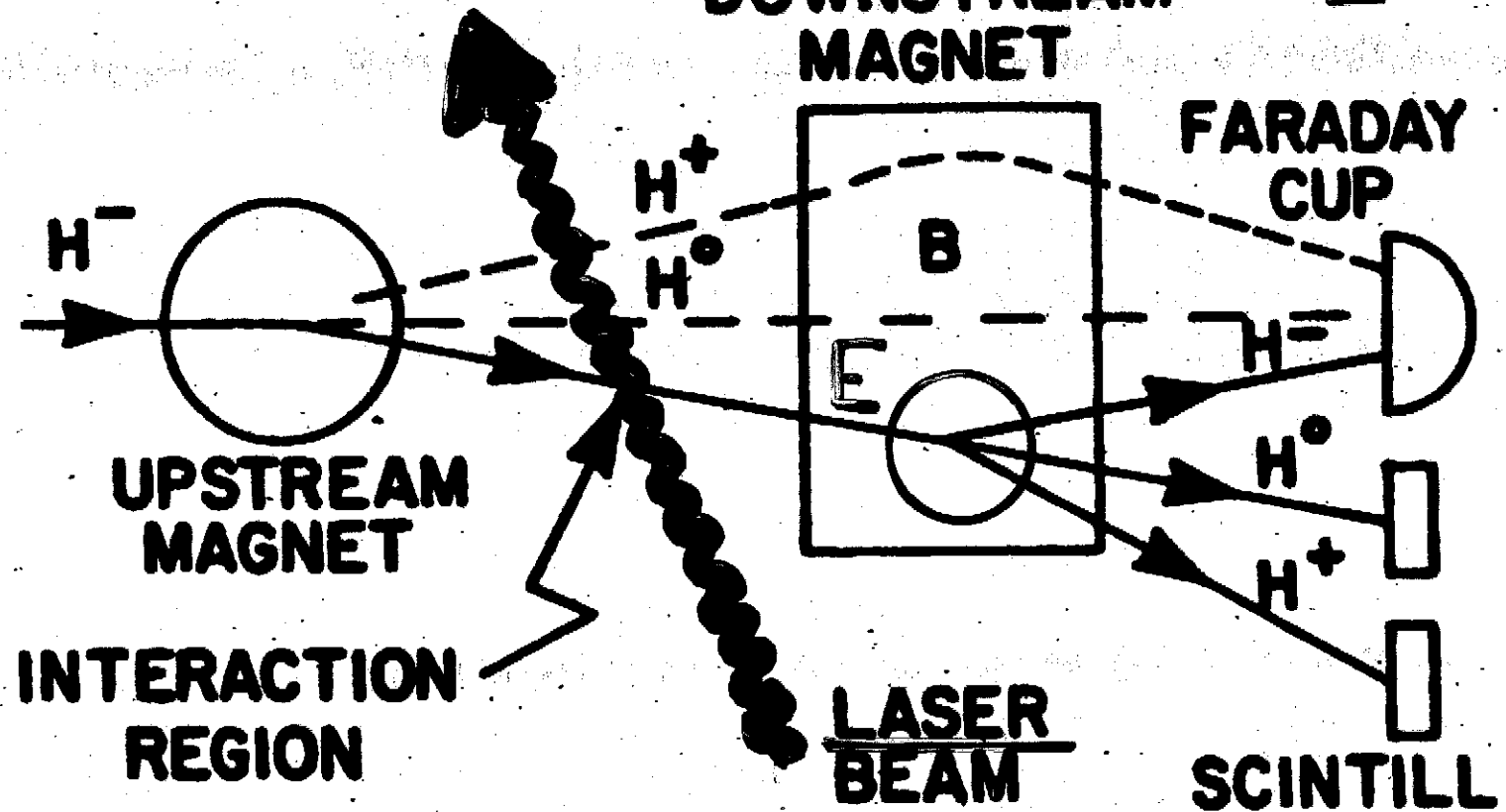


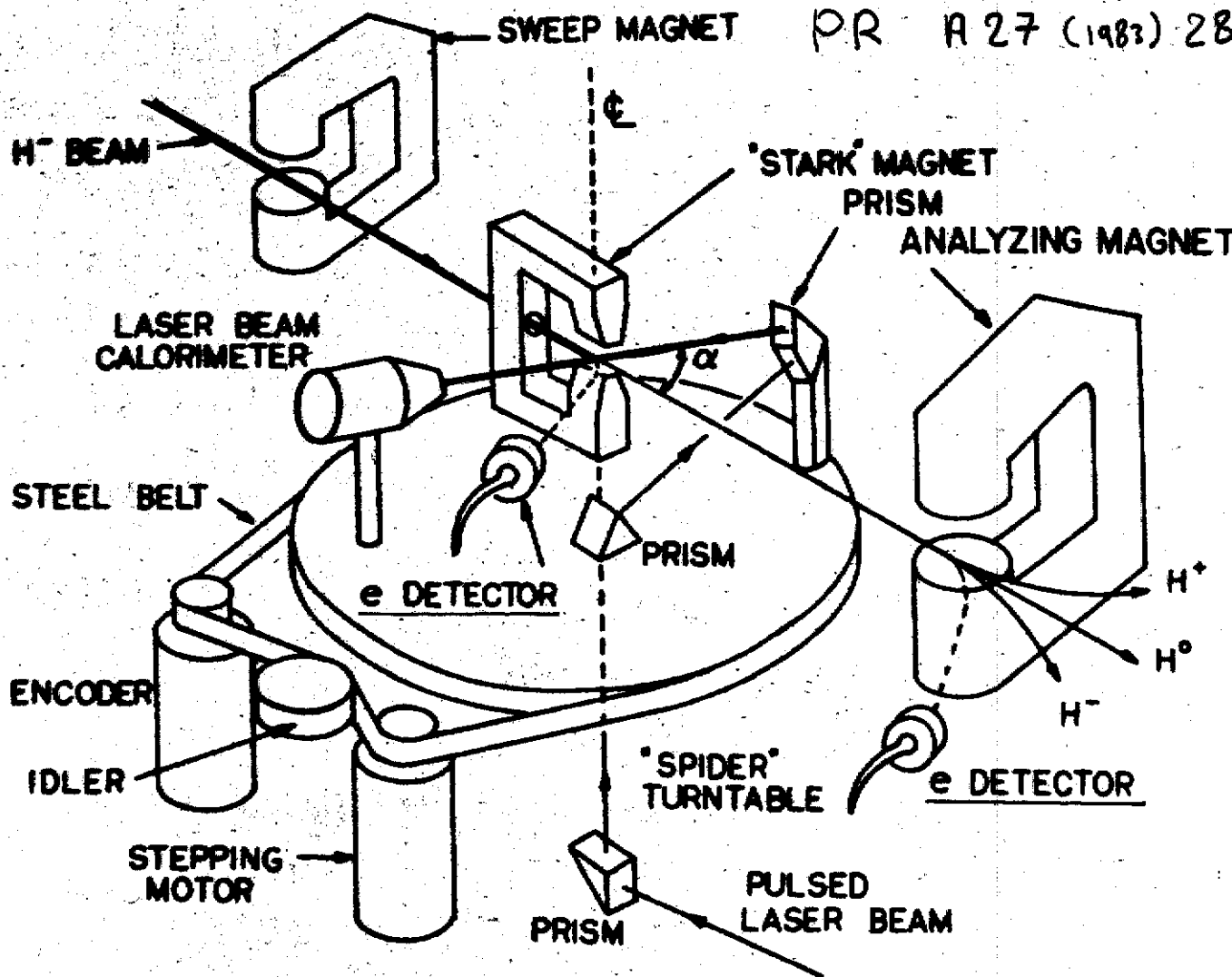
Figure 1. Schematic view of the crossed beam apparatus.

Lorenz stripping

by motional E field seen
in H^- c.m. system causing

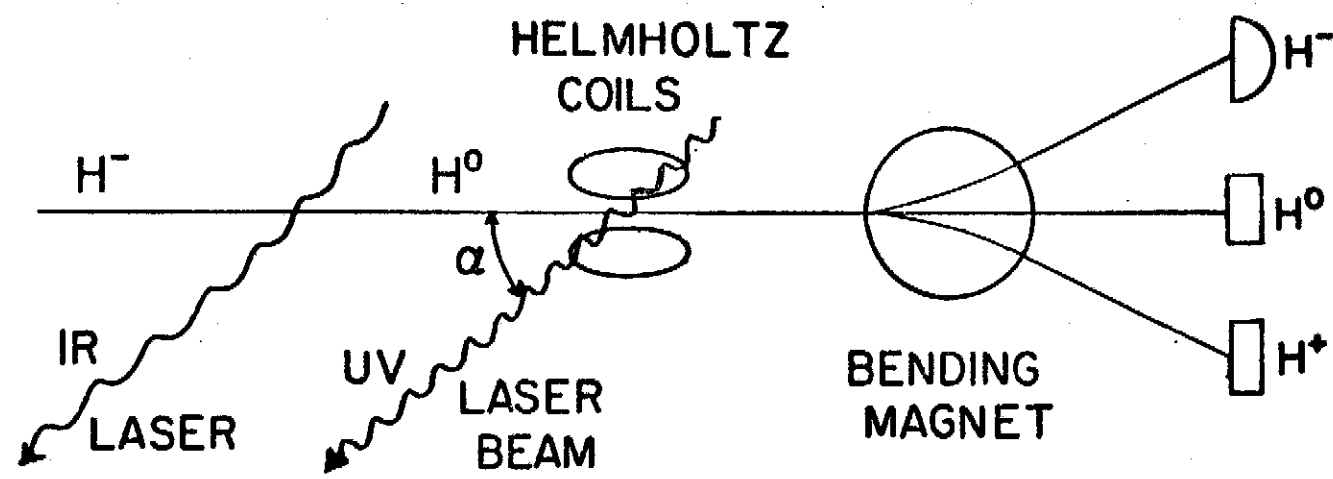
of H^0 photoexcited by Laser to
excited state

Bryant et al 1983
PR A 27 (1983) 2889



SCHEMATIC OF LAMPF PHOTODETACHMENT APPARATUS

FIG. 1. Schematic diagram of photodetachment apparatus in which a transverse magnetic field can be applied to the interaction region. 800-MeV H^- ions pass through the upstream sweep magnet to remove unwanted electrons and compensate for the bend of the analyzing magnet before they enter the main chamber. Laser beam crosses the ion beam within the poles of the interaction magnet at the center of the chamber. Magnet was orient-



$$B_{\max} \sim 0.65$$

$$E_{\text{rf}} \sim 3 \text{ MV/cm}$$

(800 MeV H⁻)

Ref 21
 Bergeman et al.
 (LAMPF)
 Atomic Physics 9

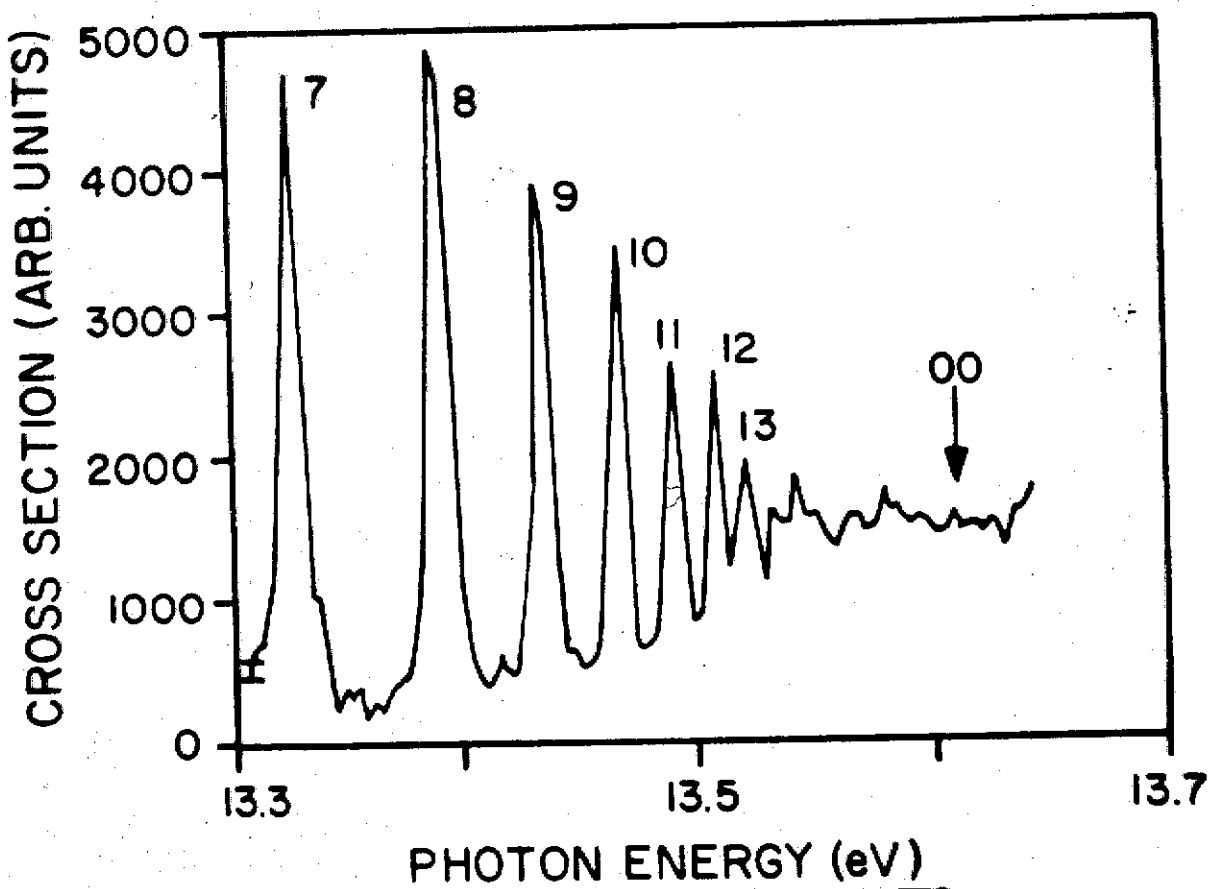
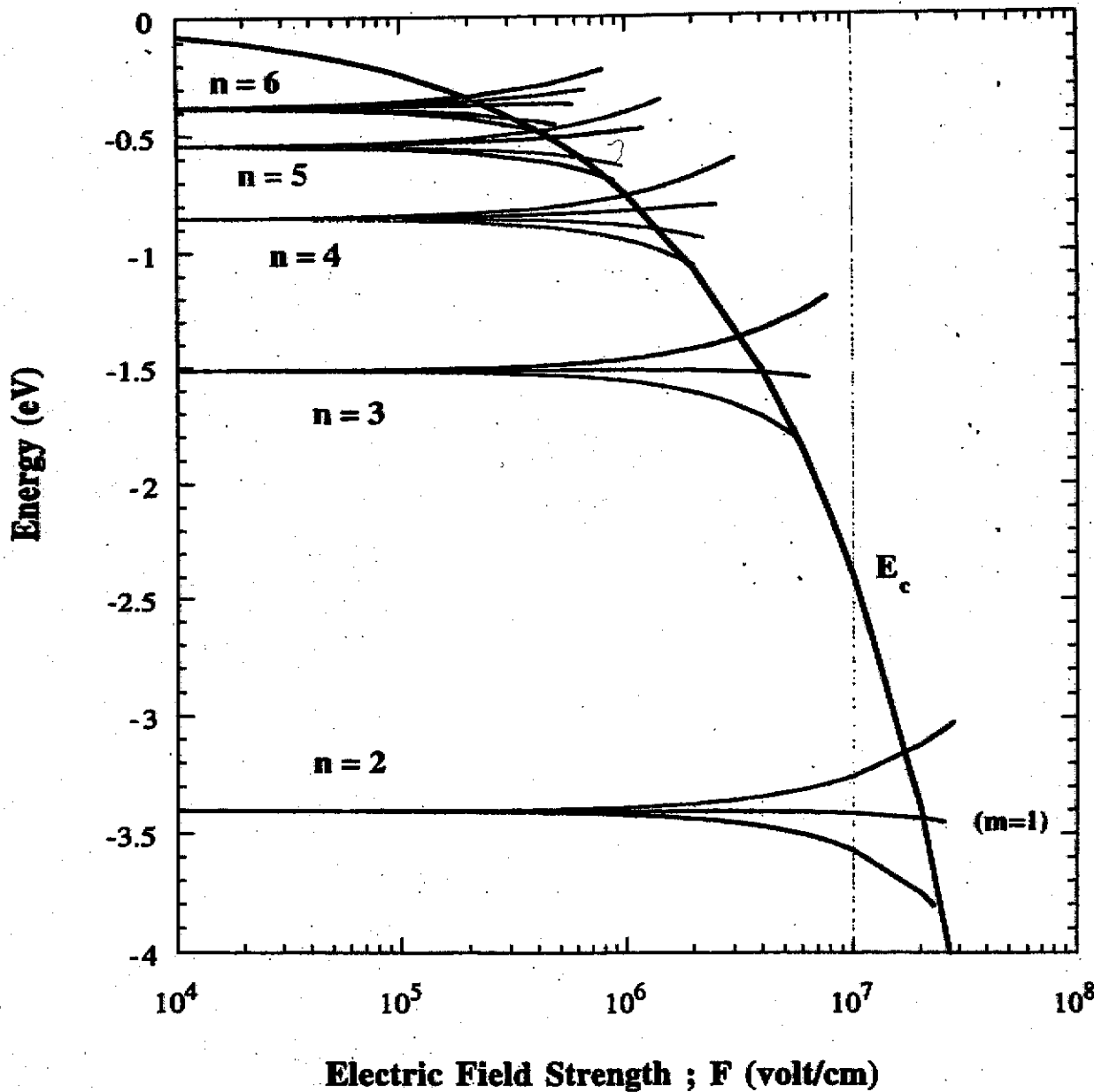


Figure 4. Photoexcitation of Lyman series in atomic hydrogen followed by stripping in a motional electric field. The numbers next to the peaks identify the principal quantum number of the state. The amplitudes follow a $1/n^3$ dependence except for $n = 7$ and $n = 8$ which are saturated.

Level Shift by Stark Effect (m=0-selected)

$$E = 27.2 \left[-\frac{1}{2n^2} + \frac{3}{2} n(k_1 - k_2) \frac{F}{5.14 \times 10^9} - \frac{1}{16} n^4 \{ 17n^2 - 3(k_1 - k_2)^2 - 9m^2 + 9 \} \frac{F^2}{(5.14 \times 10^9)^2} \right]$$

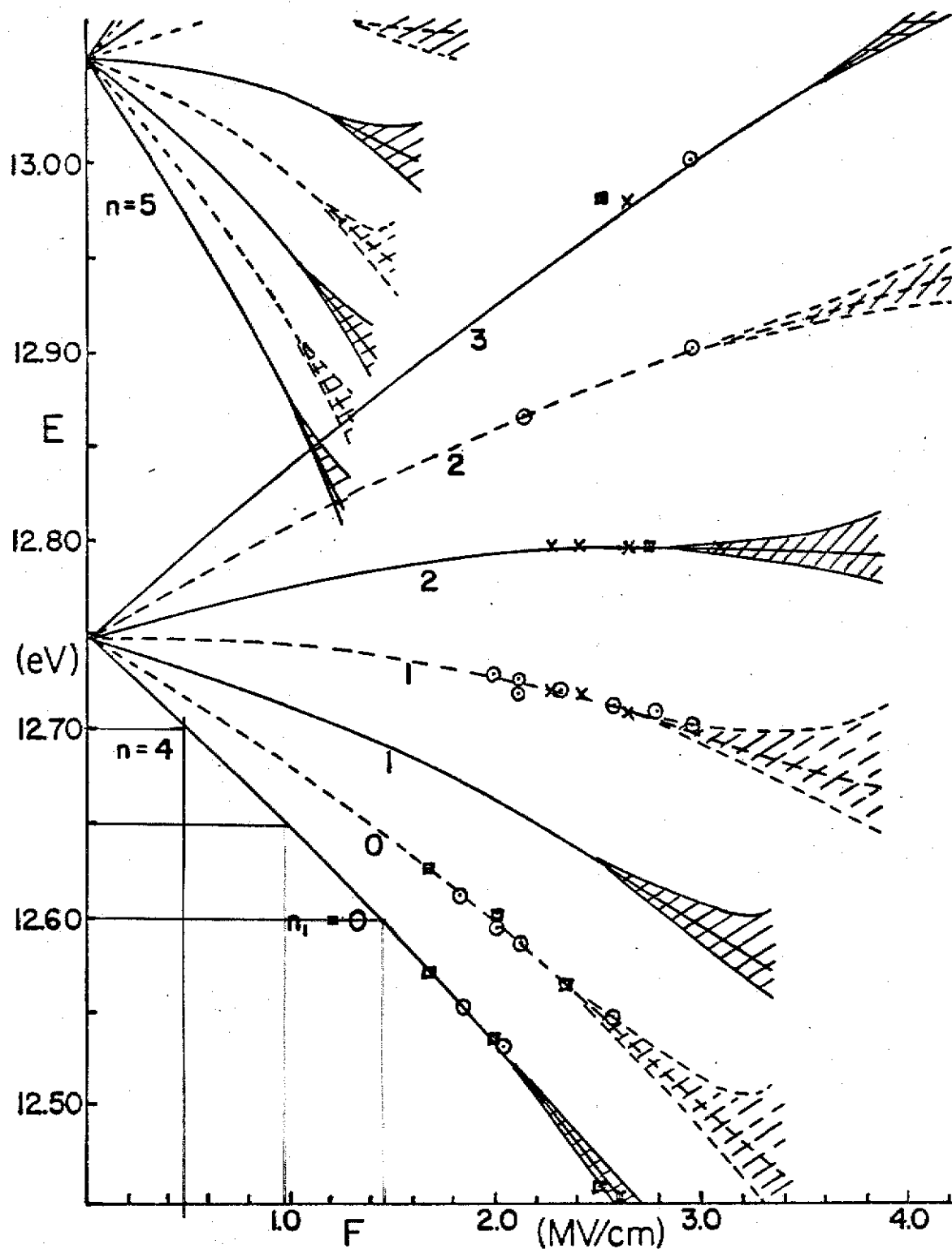


(from schematic drawing)
See B & S tef. 37
+ quantitative expt.)

~ 2 Gauss $\Rightarrow 0.1$ eV shift
 ~ 100 Gauss $\Leftarrow 0.005$ eV
 \updownarrow
 $\sim 5 \cdot 10^{-4}$ $\frac{\Delta E}{E}$

Bergeman et. al.
Atomic Physics 9
Seattle 1984

H I (11)



ref. 21

Fig. 2

Bergeman et al.

Bergeman et al.
Atomic Physics 9
Seattle 1984

H⁰(n=4)

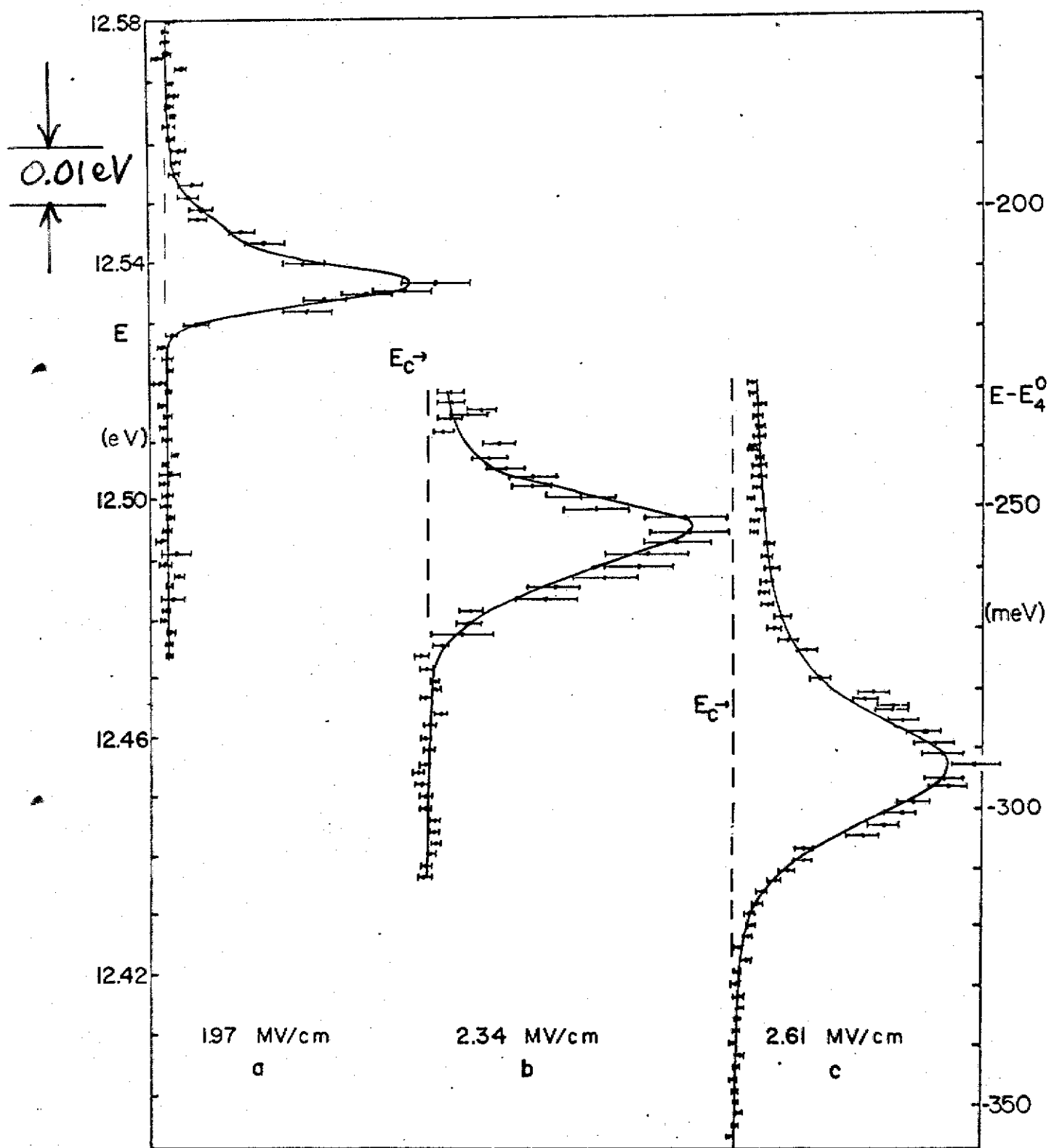


Fig 21
Bergeman et al.

31 JANUARY 1977

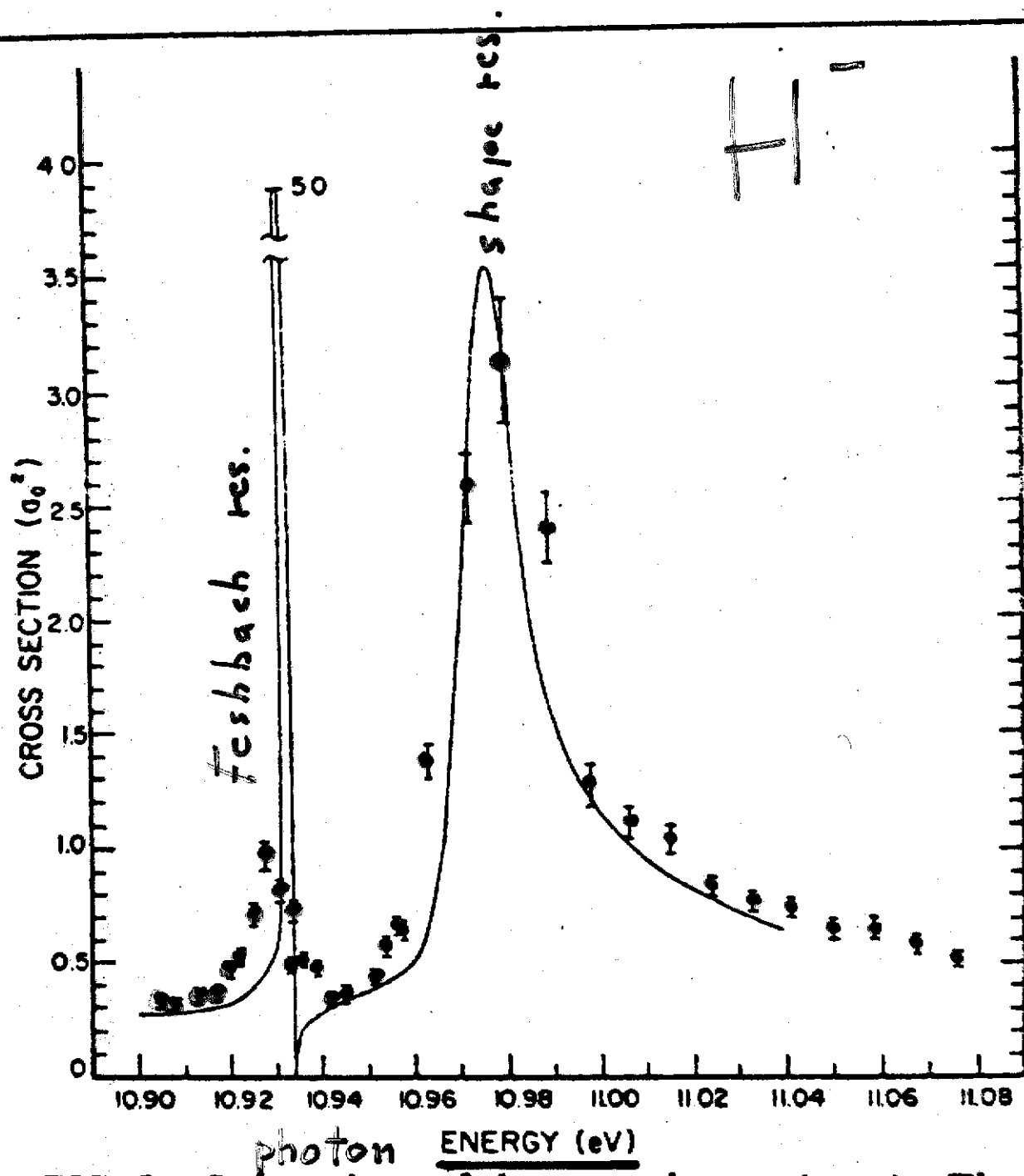
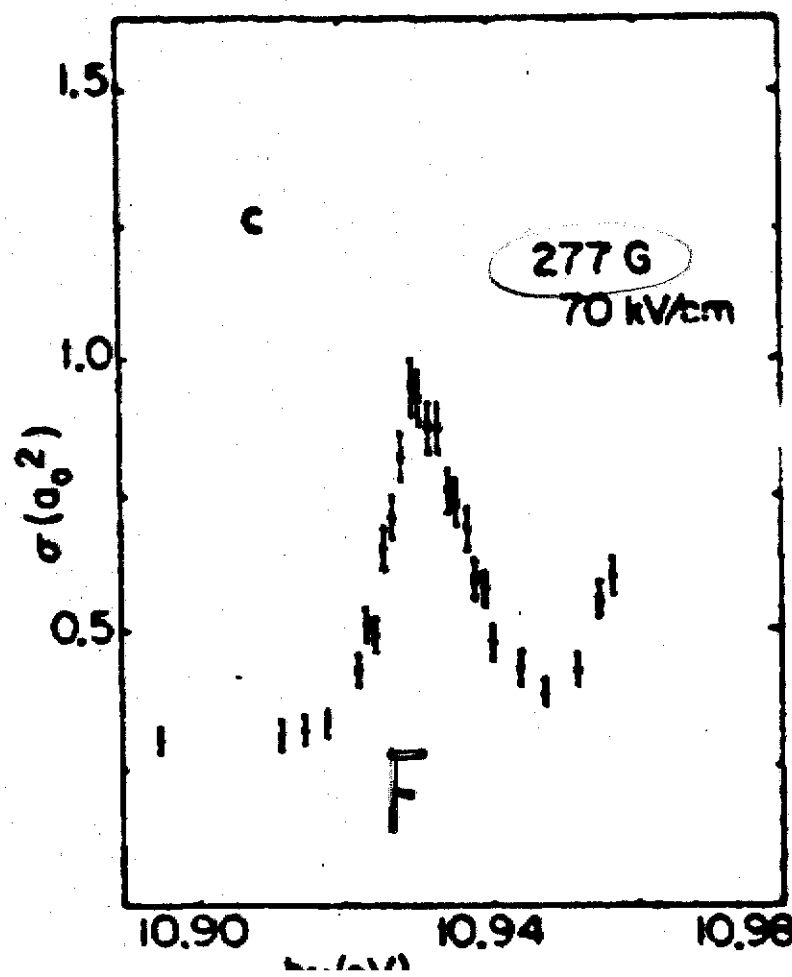
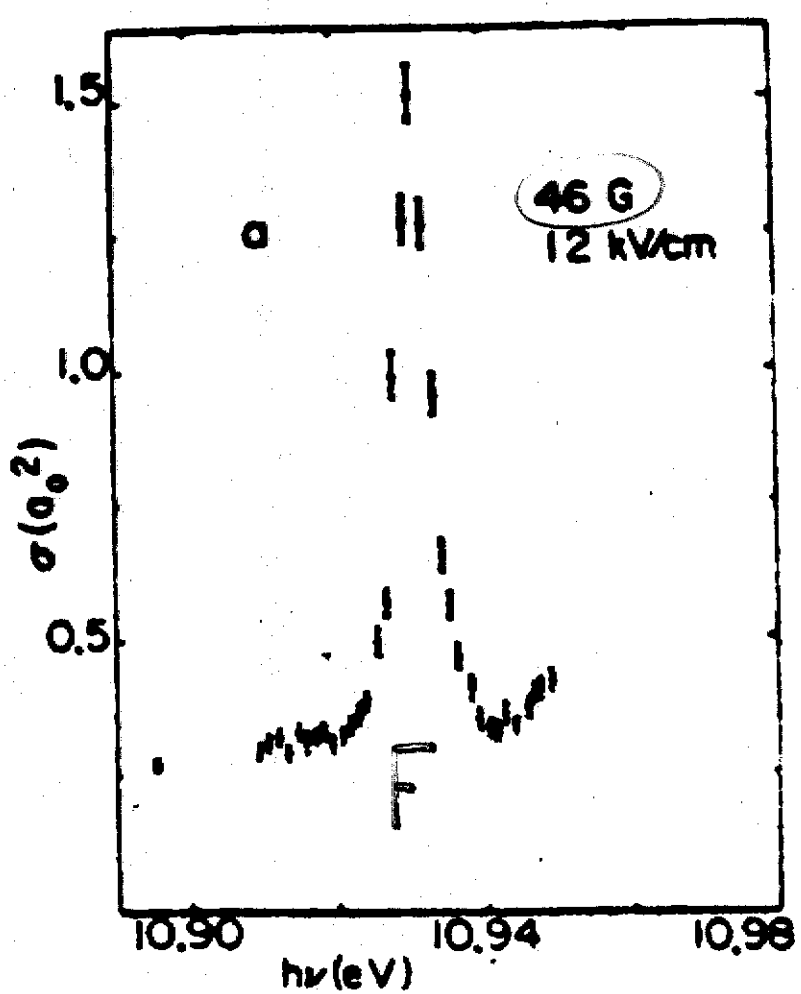


FIG. 2. Comparison of theory and experiment. The solid curve is from a calculation by Broad and Reinhardt (Ref. 1). The data points are from this experiment, normalized to theory at 10.90 eV. The error bars are statistical only.

detect e^- of E stripped H^-

Gram et al. 1978
PRL 40 (1978) 107



detect e^-

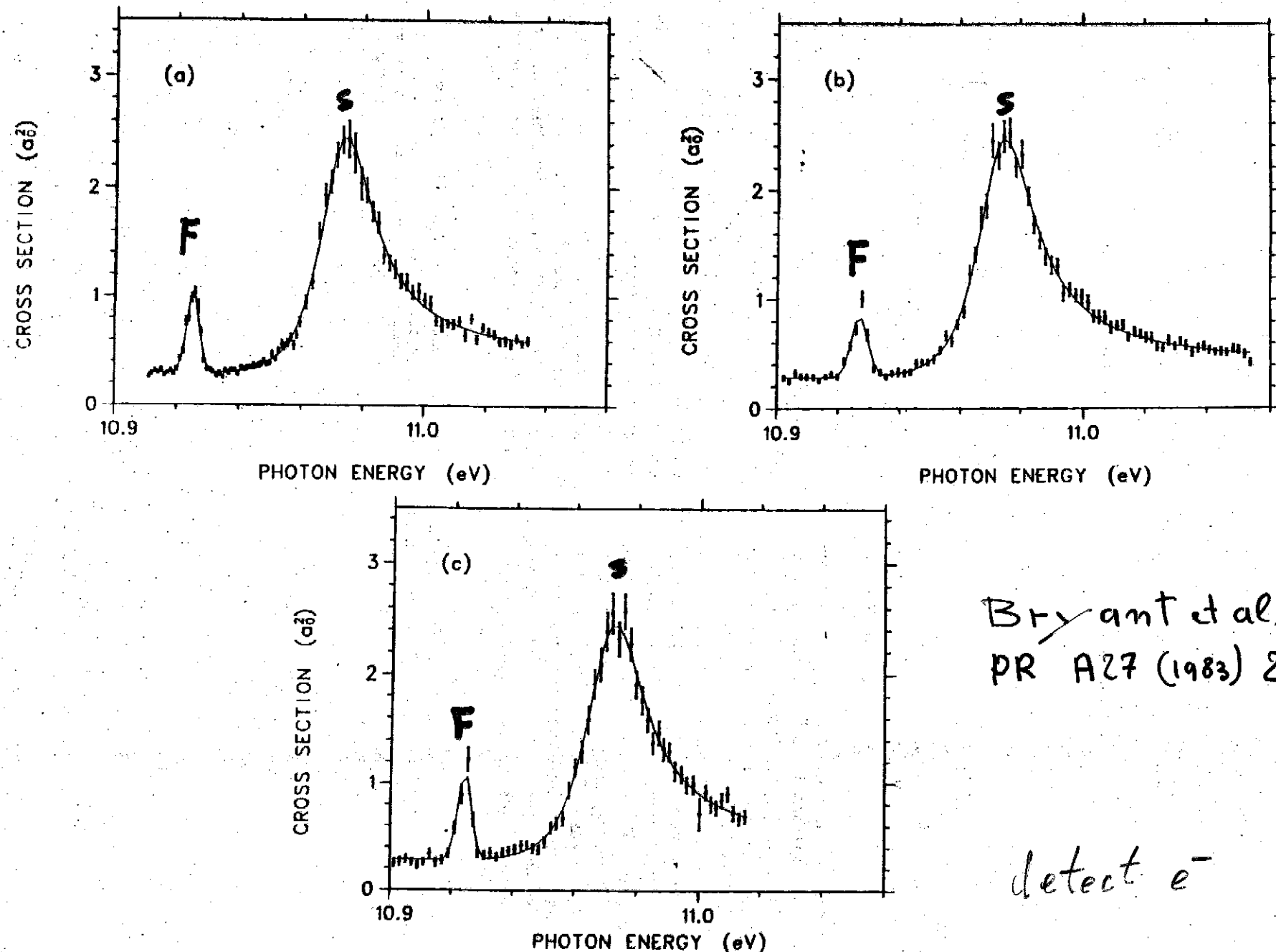


Fig. 6. Fits of data shown in Fig. 5 with Fano line shape Eq. (13) for the shape resonance and Gaussian form Eq. (14) for the 1P Feshbach resonance. See Table I. As in Fig. 5, three different runs are shown for comparison with each other. The runs for (a), (b), and (c) here correspond to Figs. 5(a), 5(b), and 5(c), respectively.

Mohagheghi et al.

PR A43 (1991) 1345

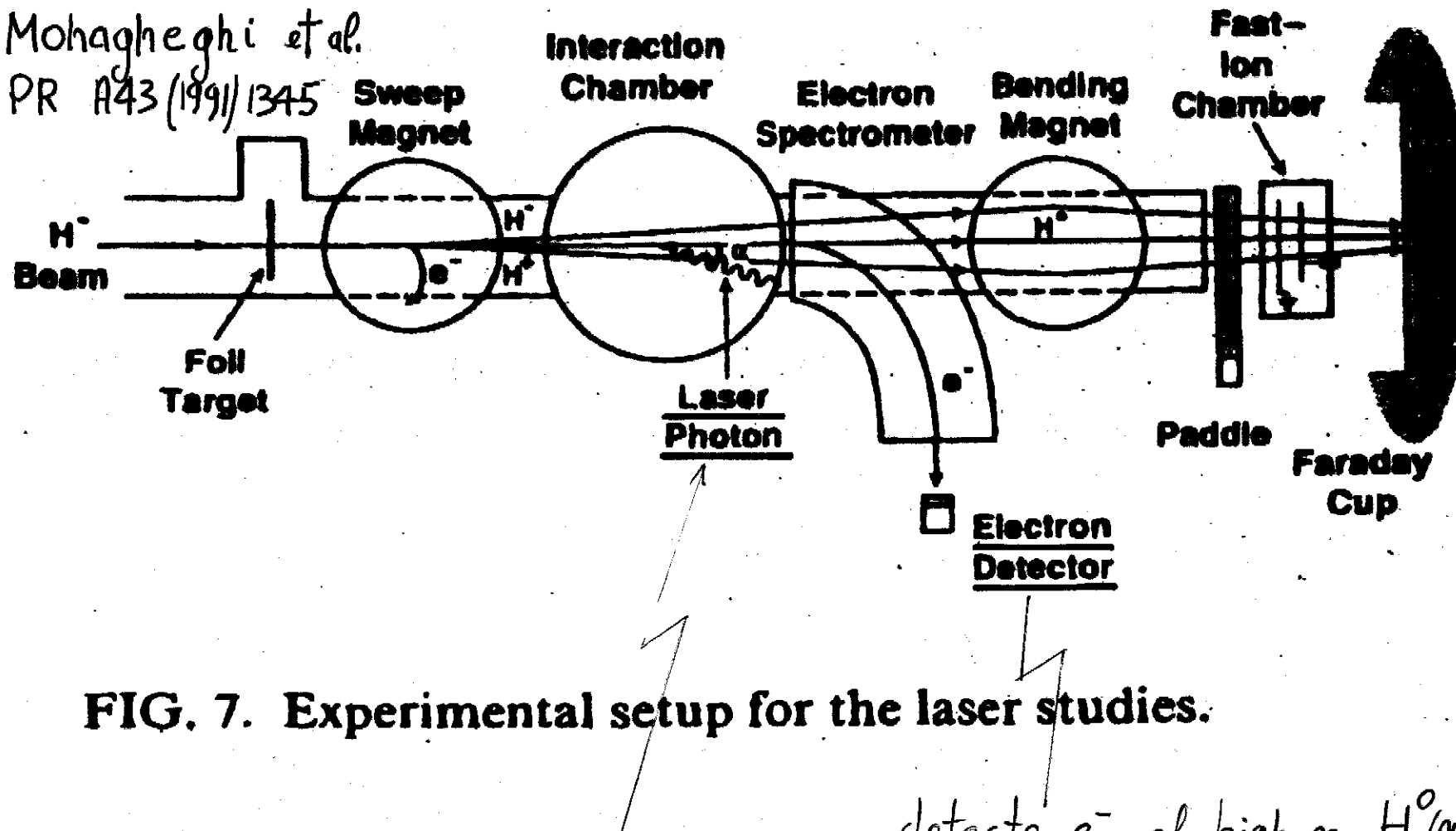


FIG. 7. Experimental setup for the laser studies.

induces transitions of
 $H^{\circ}(n=1)$ to high n $H^{\circ}(n)$

$n = \frac{1}{2}$

detects e^- of high n $H^{\circ}(n)$
Lorentz stripped in
magnetic field of e^-
spectrometer

$$\Delta p/p \downarrow \text{to } 10^{-4} \quad \Delta\theta \downarrow 10^{-6} \text{ rad, typical } 10^{-5} \text{ rad}$$

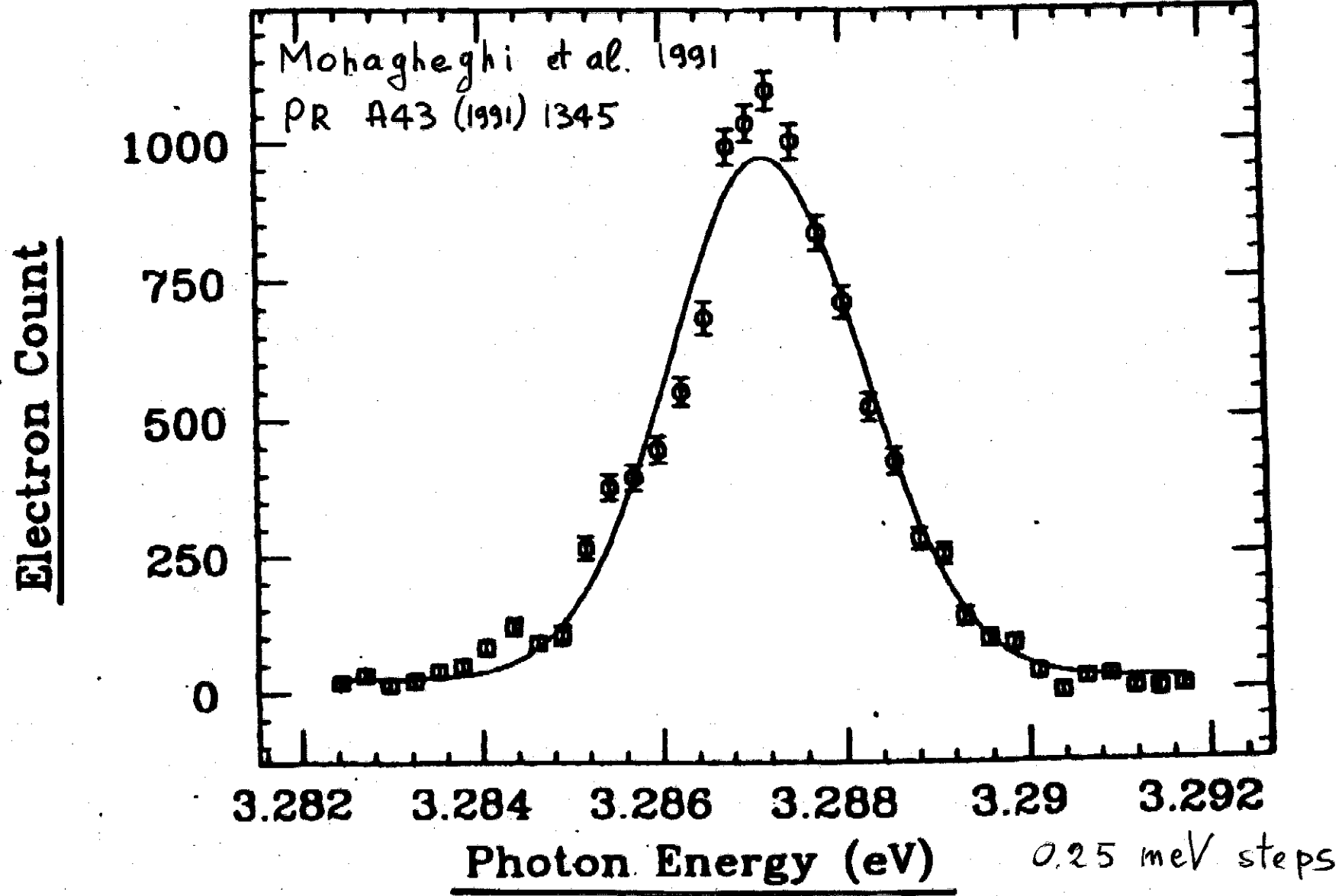


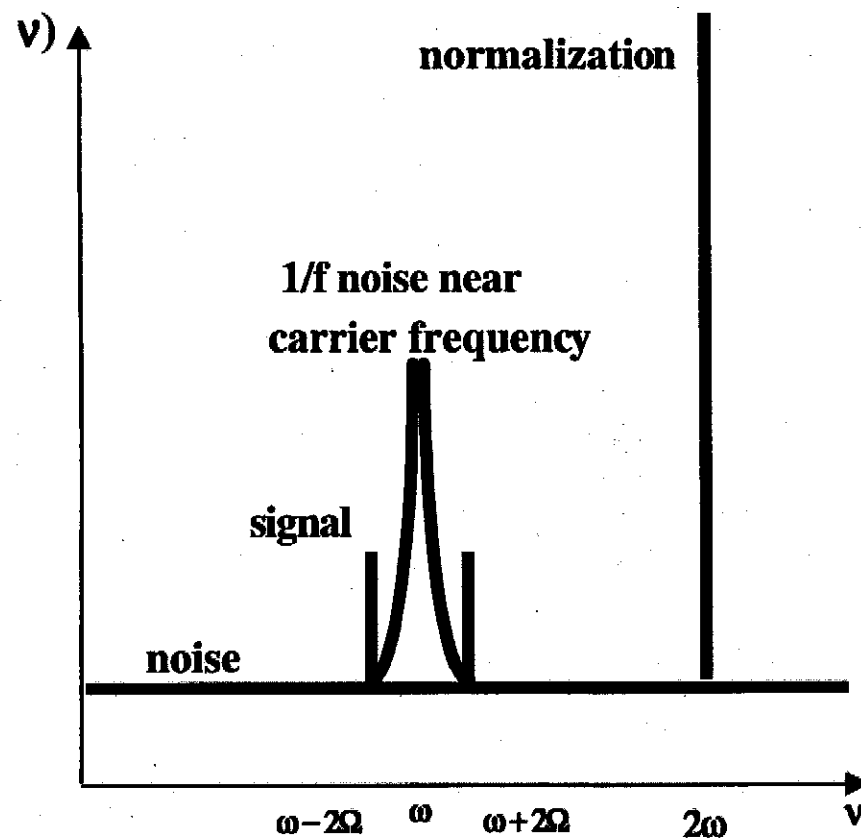
FIG. 8. $n = 2 - 11$ transition taken at 800 MeV with the fundamental wavelength (1064.4 nm) of the YAG laser.

see Cantatore et al.
ICFA HB 2002

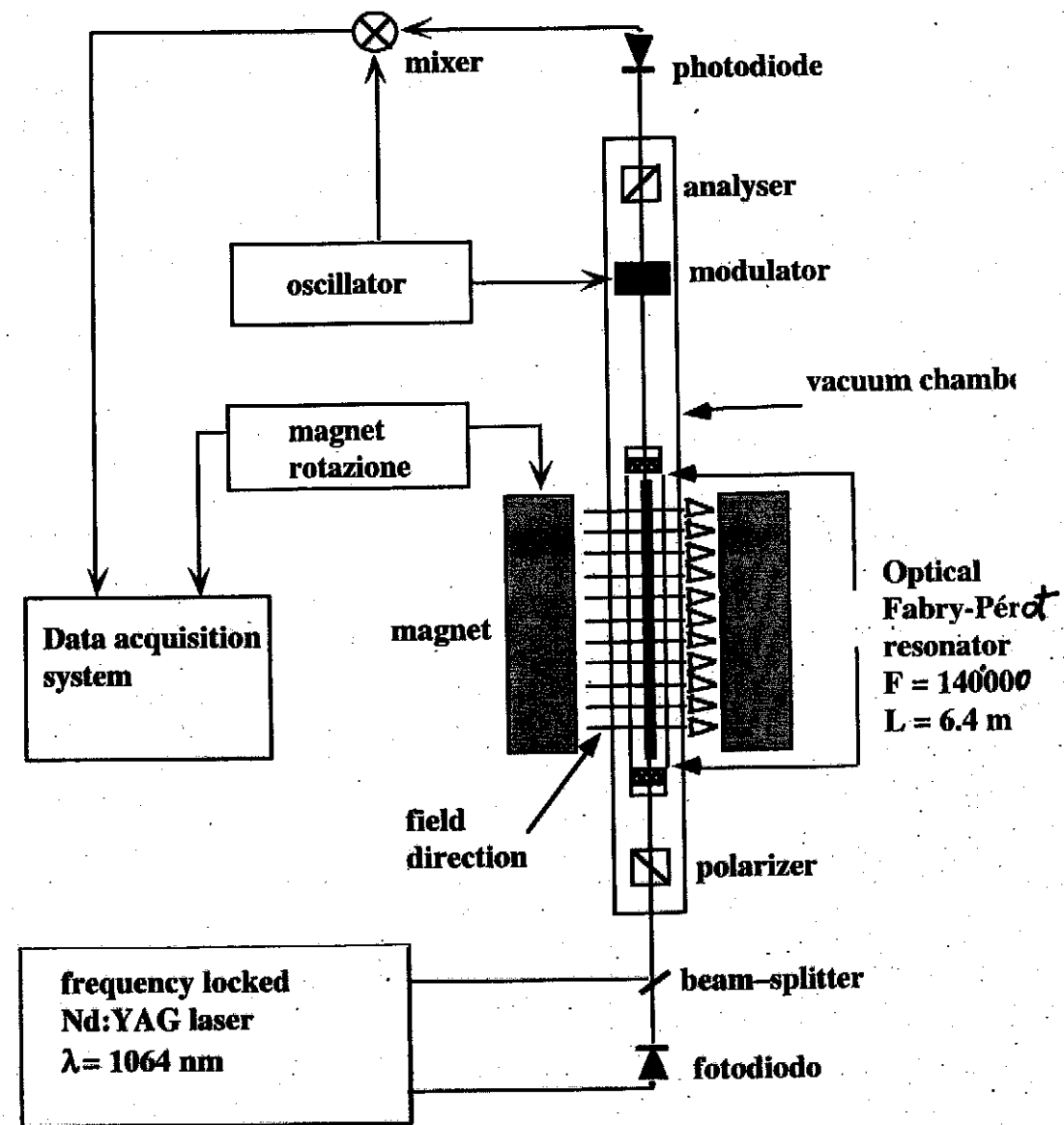
PVLAS at LNL

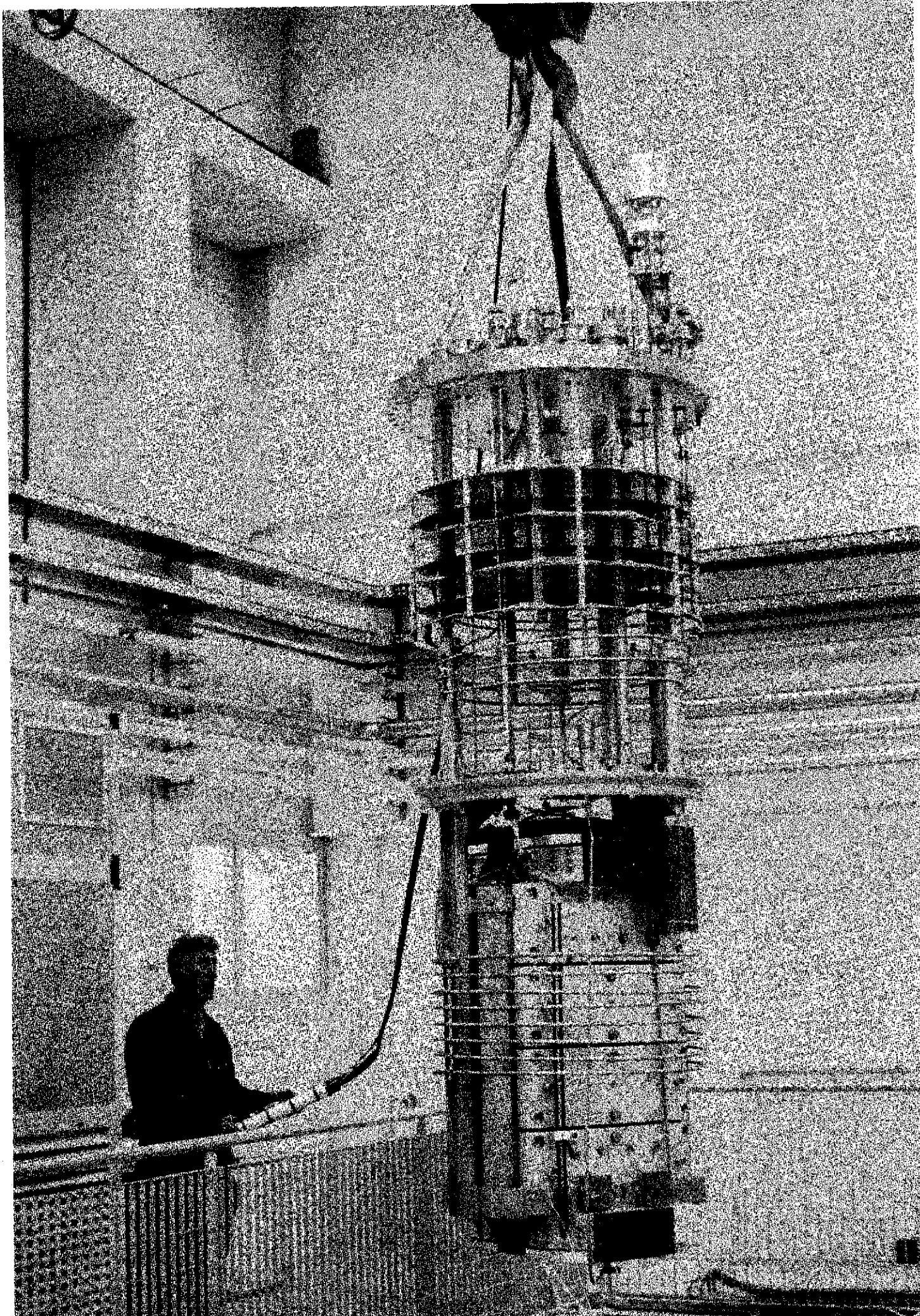
Detection scheme for light neutral (pseudo)scalar particles

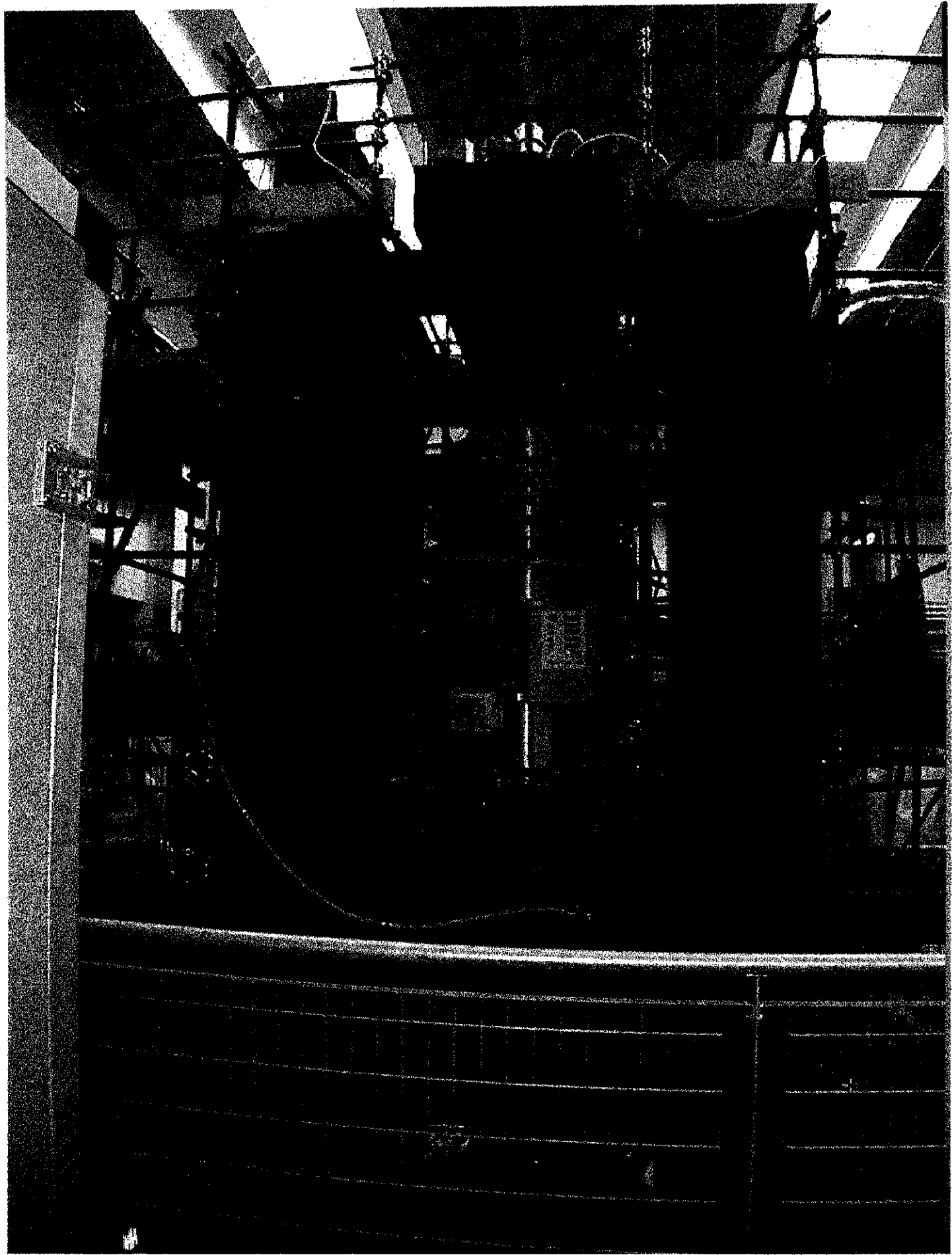
Fourier spectrum of photodiode current



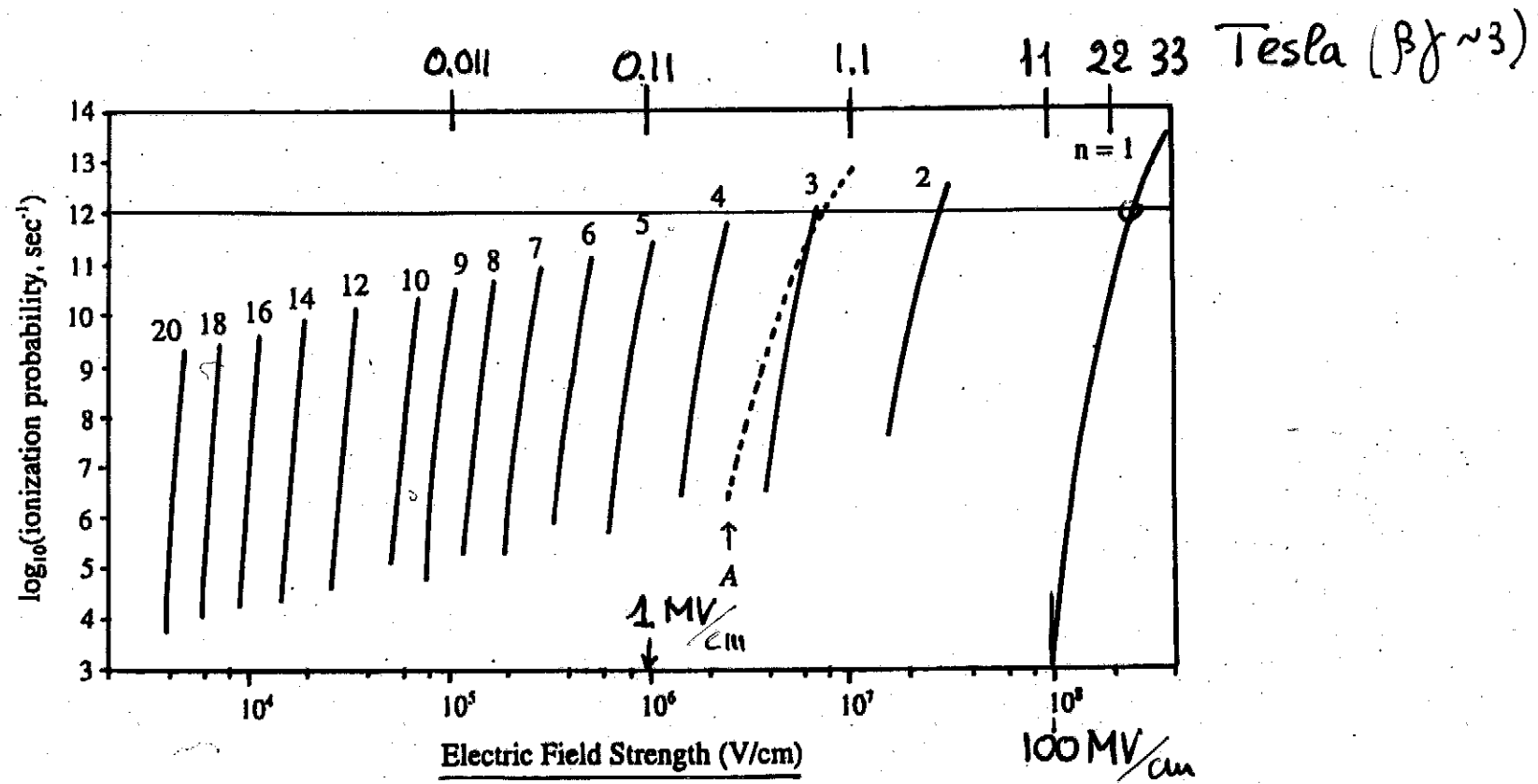
See Bakalov et al.
Q.S. Opt B 10 (1998) 329







I. YAMANE
 PR ST A&B 1(1948)
 053501-1



$$E_{rf} (\text{MV}) = 3\beta \gamma B_{Lab} (\text{T})$$

$$\beta \gamma \sim 3 \rightarrow B_{Lab} \sim \frac{E_{rf}}{g}$$

(see C. Lanczos Z.P. 1931)
 See I. Yamane & K. K.
 + g II
 M. Suzuki TAN

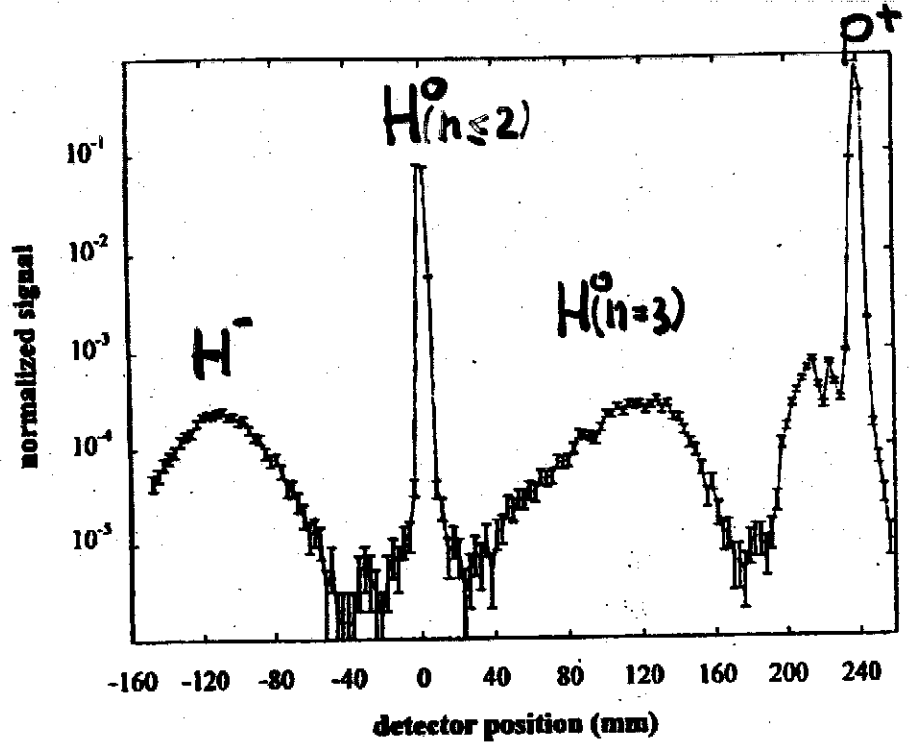


FIG. 5. Normalized signal $(H_2 \cdot S_1 \cdot S_2)/(S_1 \cdot S_2)$ vs detector position x plotted on a logarithmic scale. The error bars indicate the standard deviations for each data point. The Gypsy magnet was set to a peak field of 1.3 T to separate the $n = 3$ level from those of higher n . The FIF magnet was set to 0.16 T. The broad feature peaked near -100 mm is due to field-detached H^- , the narrow peak at $x = 0$ is due to unstripped H^0 , and the broad feature peaked near 120 mm is due to field-stripped $n = 3$ states. The peak due to protons is centered near 240 mm and the shoulder appearing on the lower- x -value side of the H^+ peak is due to field ionization of H^0 states in levels $n > 3$.

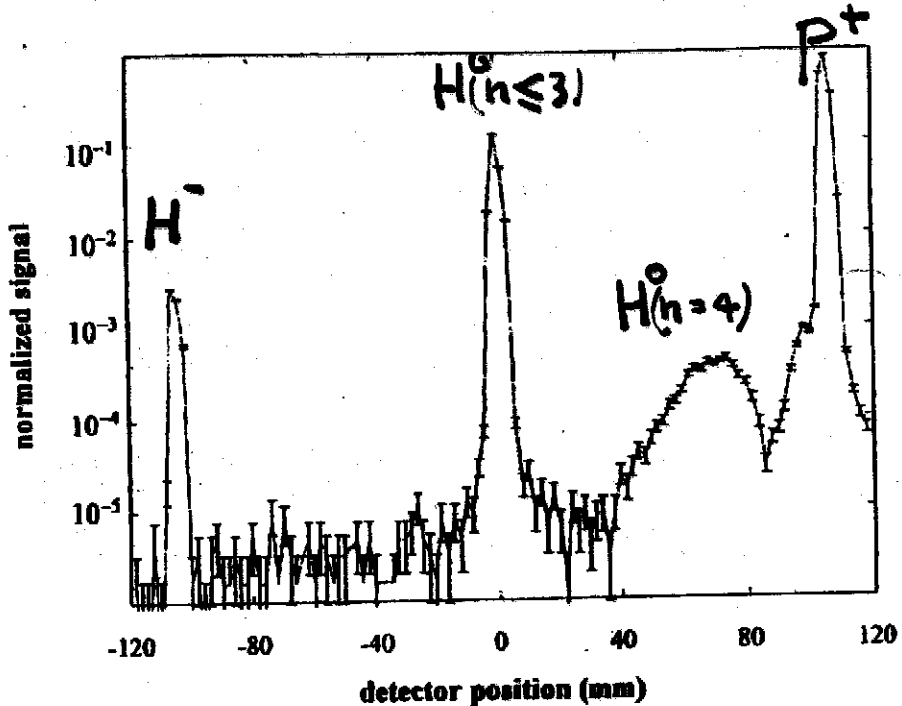


FIG. 16. Normalized signal $(H_1 \cdot S_1 \cdot S_2)/(S_1 \cdot S_2)$ vs x obtained with the Gypsy magnet set to a peak field of 0.6 T to separate the $n = 4$ level from those of higher n . The FIF magnet was turned off. The error bars indicate the standard deviations for each data point. The shoulder beginning near 90 mm is due to ionization of H^0 states in levels $n > 4$.

Keating et al. 1998
PR A 58 (1998) 4526

detect p⁺

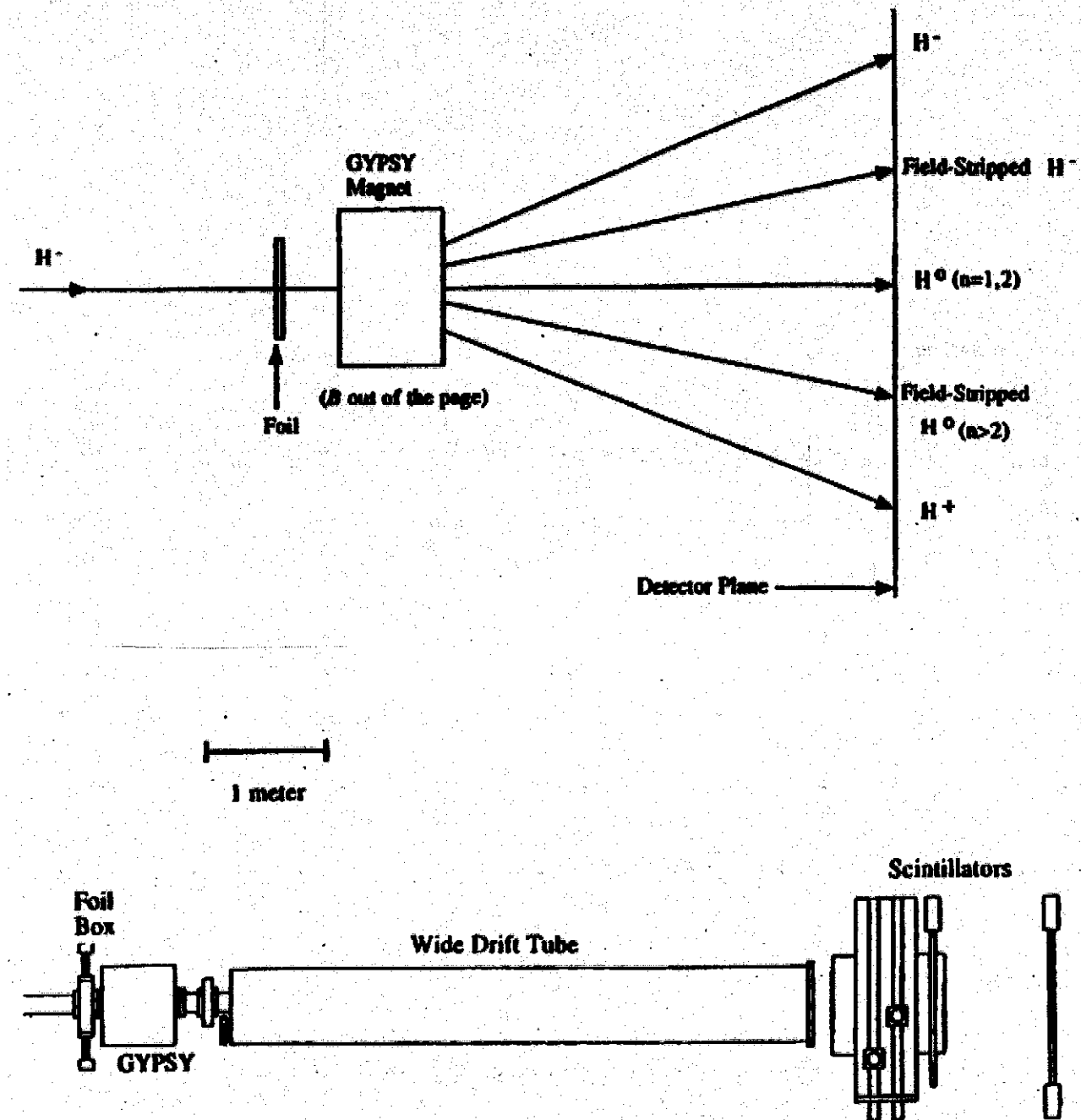


FIG. 3. The 800-MeV H^- beam is directed through a self-supported 2-cm-diam foil. The emerging excited states of hydrogen are sorted by the gradient-field magnet (labeled "gypsy" magnet); their trajectories reflect the strength of the required stripping field. H^0 ($n = 1$ and 2) cannot be stripped by the field. Unstripped H^- and fully stripped H^+ are deflected maximally.

Gulley et al. 1996
P.R. A53 (1996) 3201

FIG. 4. The H^- beam enters from the left. Any one of an assortment of foils is inserted into the beam by means of remotely operated actuators in the foil box. After emerging from the gypsy magnet the various hydrogenic charge states drift in a vacuum of 10^{-7} torr for 5.3 m before striking the exit window, where they are completely stripped, and passing through the scintillator telescope. One of two scanning pencil scintillators is used to trace out the distribution of particles.

detect p⁺

Keating et al. 1998
PR A58 (1998) 4526

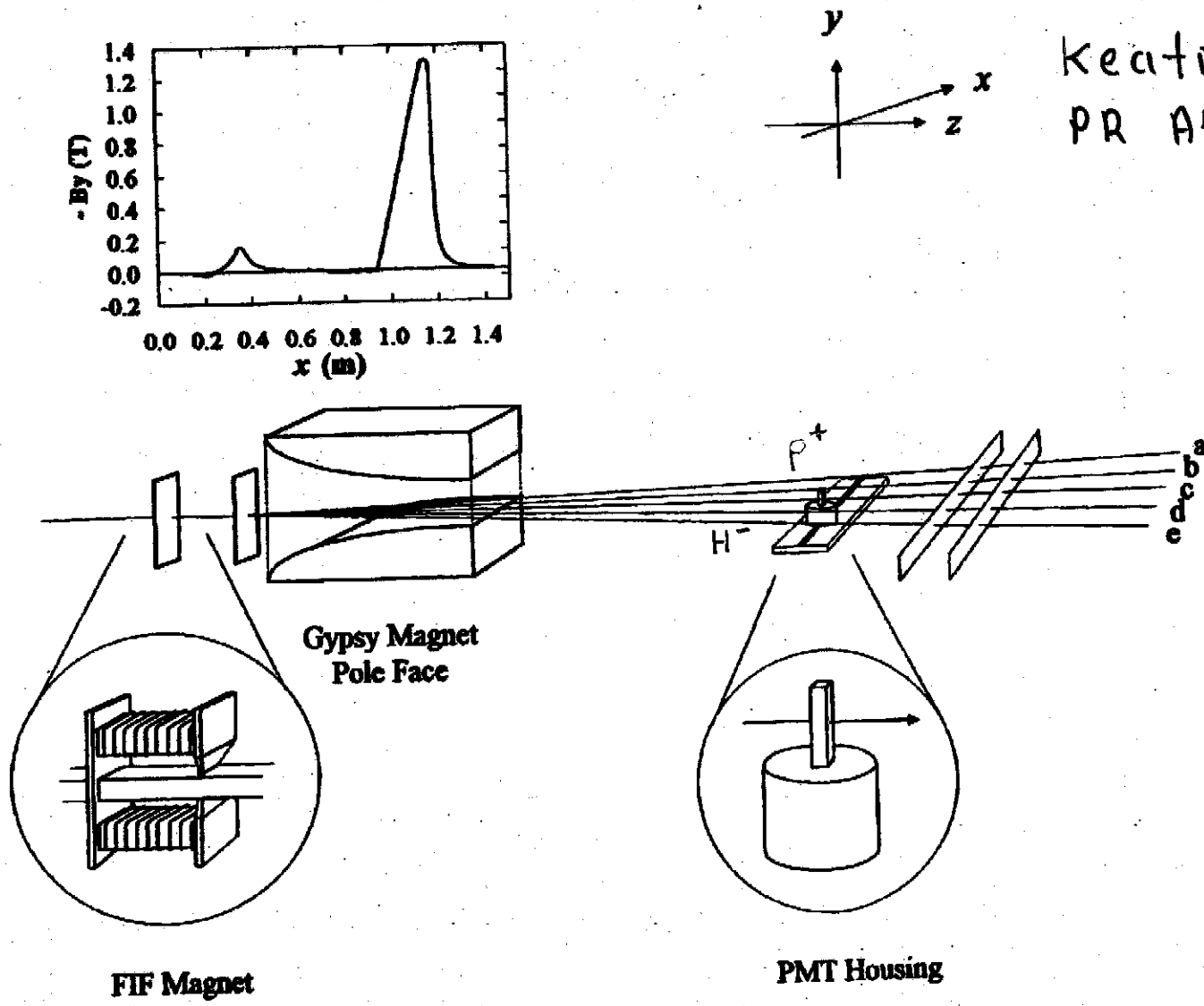
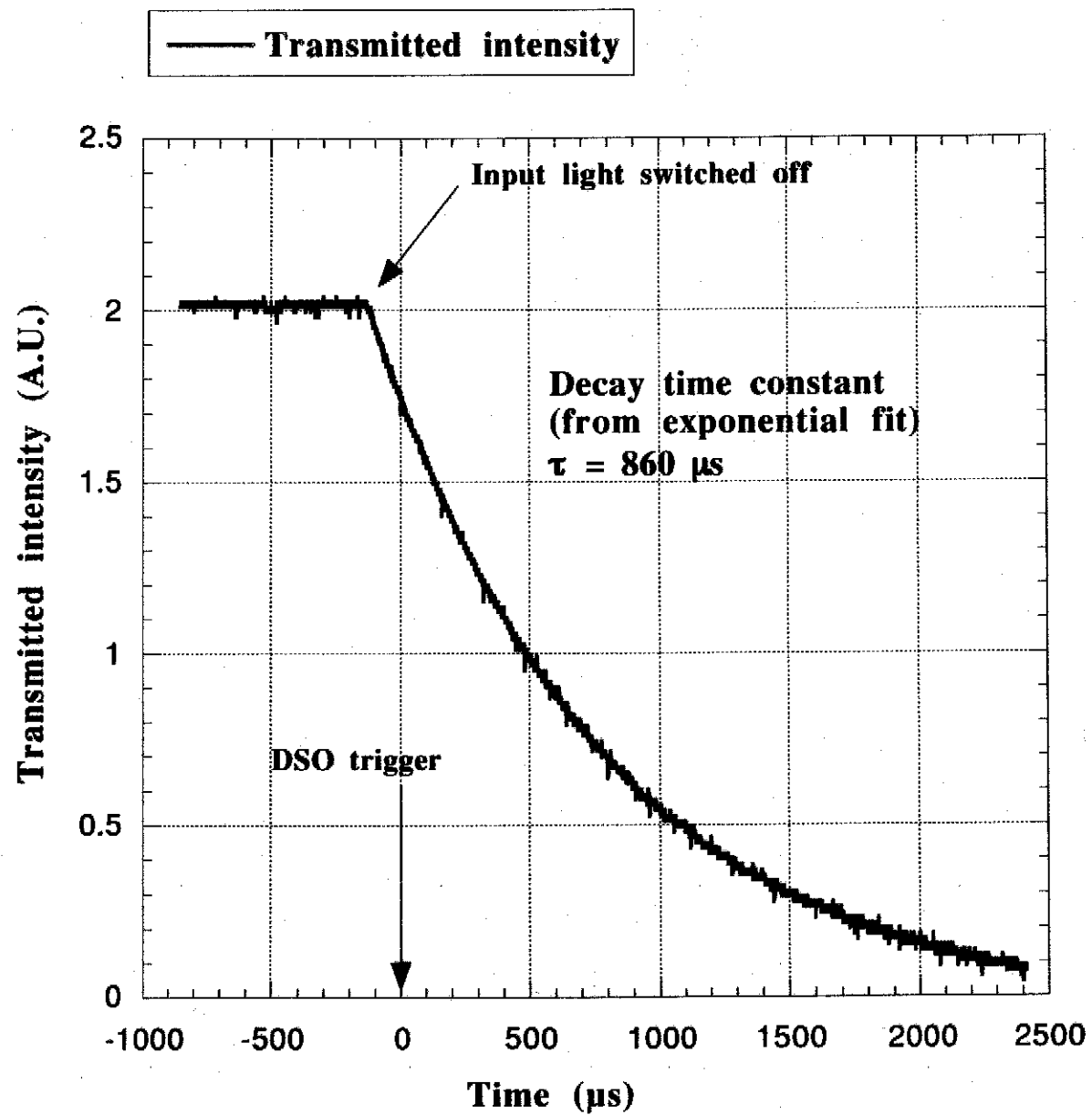
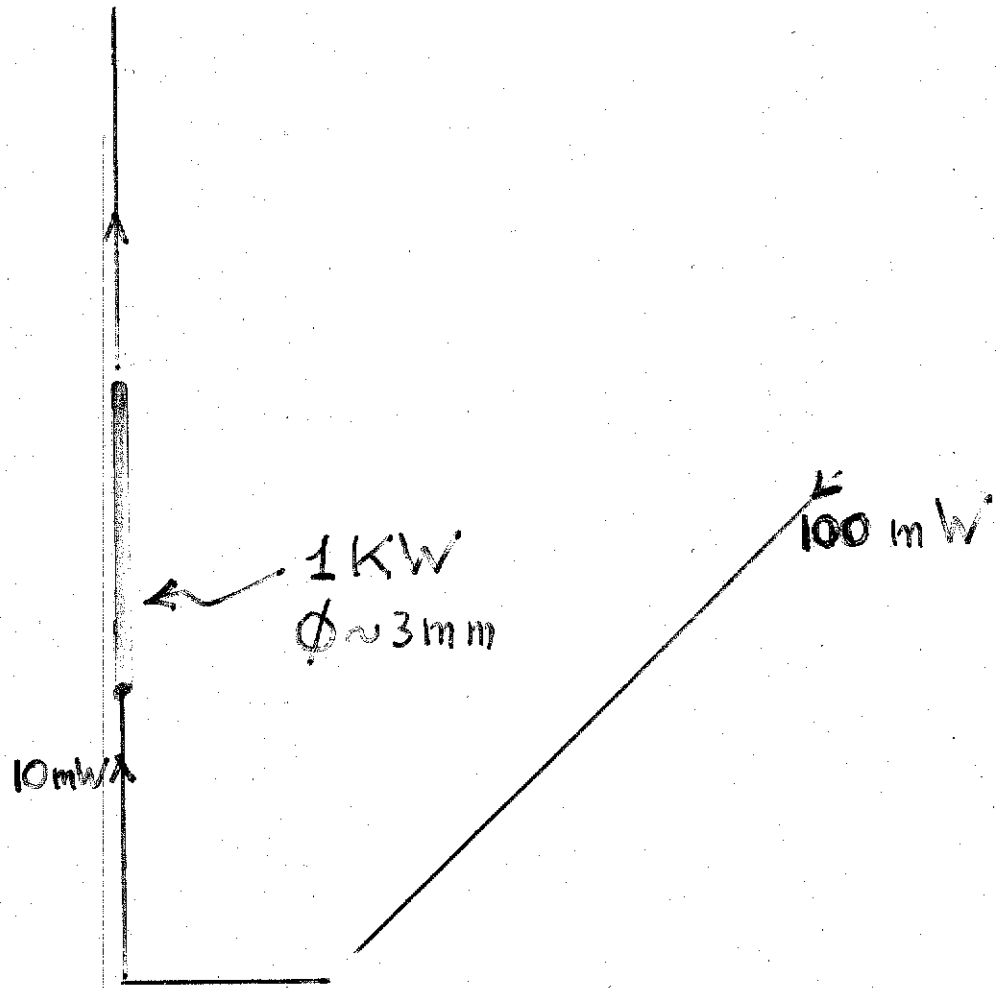


FIG. 4. Diagram showing the possible outcomes of interactions of H^- , H^0 , and H^+ with the foil and "Gypsy" magnet. The various charge states are separated and detected 5.5 m from the peak magnetic field with a scanning scintillator in coincidence with two wide scintillators. The scanning scintillator travels along the x direction, both magnetic fields point in the negative y direction, and the incident beam defines the z direction. An aluminum window at the end of the drift tube (not shown) strips all electrons from H^0 and H^- so that only protons are detected. Protons that enter the Gypsy magnet are detected at position a and protons derived from field-detached H^- and H^0 states not field stripped, field-stripped H^0 states, and H^- not field detached appear at positions b , c , d , and e , respectively. PMT denotes photomultiplier tube.

detect p^+





$$10 \text{ mW} \rightarrow 1 \text{ KW}$$

$$10^{-2} \rightarrow 10^3 \text{ kW}$$

gain 10^5

$$100 \text{ mW laser} \rightarrow \sim 6 \cdot 10^{17} \text{ 1ev photons}$$

Laser delivers to FP $\sim 6 \cdot 10^{16} \text{ ph sec}^{-1}$
 $(\sim 10^3 \text{ of laser photons enter MM})$

permanently present inside FP $\sim 6 \cdot 10^{16} \text{ photons}$

rate of Laser induced transitions in H^0 c.m.
at resonance frequency, in level NOT broadened by Stark effect

Rate of laser atom transitions in H^0 c.m. at resonance width in level NOT broadened by Stark effect at a width

$$\Delta V \approx \Delta V = \frac{1}{\hbar} (1 - n^{-2}) R_y \frac{N P}{P}$$

$$\text{Stark } \approx \frac{a_0^2 n^{-3}}{4 \pi^2}$$

$$\text{c.m. } \approx \frac{\gamma^2 (1 + \beta \cos \alpha)^2}{n, 0, n-1, 0}$$

$$\text{Laser } \approx \frac{\gamma^2 (1 + \beta \cos \alpha)^2 I_{\text{lab}}}{I_{\text{laser}}} \sim \frac{6 \text{ cm}}{10^4 n^{-3}}$$

$$\text{natural width } \approx 5 \cdot 10^9 n^{-3} \text{ s}^{-1}$$

absence of Stark broadening

$$\Delta V \text{ STARK } \approx \frac{15}{4.5} \frac{I_{\text{lab}}}{I_{\text{FP}}} \frac{10^{15} \text{ s}^{-1} \Delta P}{P}$$

$$\text{Laser } \approx \frac{I_{\text{lab}}}{I_{\text{laser}}} \cdot \frac{1}{\gamma^2 (1 + \beta \cos \alpha)^2} \cdot \frac{1}{\left[\frac{I_{\text{lab}}}{I_{\text{FP}}} \right] \left[\frac{\Delta P}{P} \right]} \left[\frac{\text{W}}{\text{cm}^2} \right]$$

Doppler SPREAD ΔV of resonance frequency is

$$\Delta V \approx \frac{1}{\hbar} \left(1 - \frac{1}{n^2} \right) R_y \cdot \frac{\Delta P}{P} \approx 2.5 \cdot 10^{15} \text{ s}^{-1} \frac{\Delta P}{P}$$

Length L of interaction region needed to have all H^0 's within $\Delta P_{\text{start}} \approx \Delta P_{\text{laser}} + \Delta P$ crossing resonance

$$L = \frac{\Delta V}{\Delta V_{n, 0, n-1}} \approx 3 \cdot 10^6 \text{ cm} \frac{\Delta P}{P} \frac{n^3}{\gamma (1 + \beta \cos \alpha)} \frac{1}{I_{\text{FP}} \text{ [W/cm}^2\text{]}}$$

$$L_{1\lambda} = \frac{\Delta v_0}{\Delta v_m} \lambda^{\text{lab}} \simeq 3 \cdot 10^6 \text{ cm} \frac{\Delta p}{p} \frac{n^3}{(1+\beta \cos \alpha)} \frac{1}{I_{FP} [\text{KW/cm}^2]}$$

- pessimistic scenario at $\gamma \sim 3$

$$\Delta p/p = 10^{-3} \quad \gamma \sim 3 \quad (1+\beta \cos \alpha) \sim 2 \quad I_{FP} \sim 1 \text{ KW/cm}^2$$

$n = 4$

$$L_{1\lambda} \simeq 3 \cdot 10^4 \text{ cm} = 300 \text{ m}$$

$$V_{FP} = 532 \text{ nm}$$

2^{nd} atm.

$N_e > A_E$

- optimized scenario at $\gamma \sim 3$

$$\Delta p/p \simeq 10^{-4} \quad \gamma = 3 \quad (1+\beta \cos \alpha) \sim 2 \quad n = 4 \quad I_{FP} \sim 10 \text{ KW/cm}^2$$

$$L_{1\lambda} \simeq 3 \text{ m}$$

$$V_{FP} = 532 \text{ nm}$$

2^{nd} atm

$N_e > A_E$

- optimistic scenario at $\gamma \sim 3$

$$\Delta p/p \sim 10^{-4} \quad \gamma = 3 \quad (1+\beta \cos \alpha) \sim 2 \quad n = 4 \quad I_{FP} \sim 100 \text{ KW/cm}^2$$

$$L_{1\lambda} \simeq 30 \text{ cm}$$

$$V_{FP} = 532 \text{ nm}$$

2^{nd} atm

$N_e > A_E$

possible?

- plausible scenario at $\gamma \sim 6$

$$\Delta p/p \sim 3 \cdot 10^{-4}, \quad \gamma \sim 6, \quad (1+\beta \cos \alpha) \sim 2 \quad n = 4 \quad I_{FP} \sim 100 \text{ KW/cm}^2$$

$$L_{1\lambda} \simeq 50 \text{ cm}$$

$$V_{FP} = 1064 \text{ nm}$$

1^{st} atm

$N_e > A_E$

PVI AS: 10 KW/cm^2

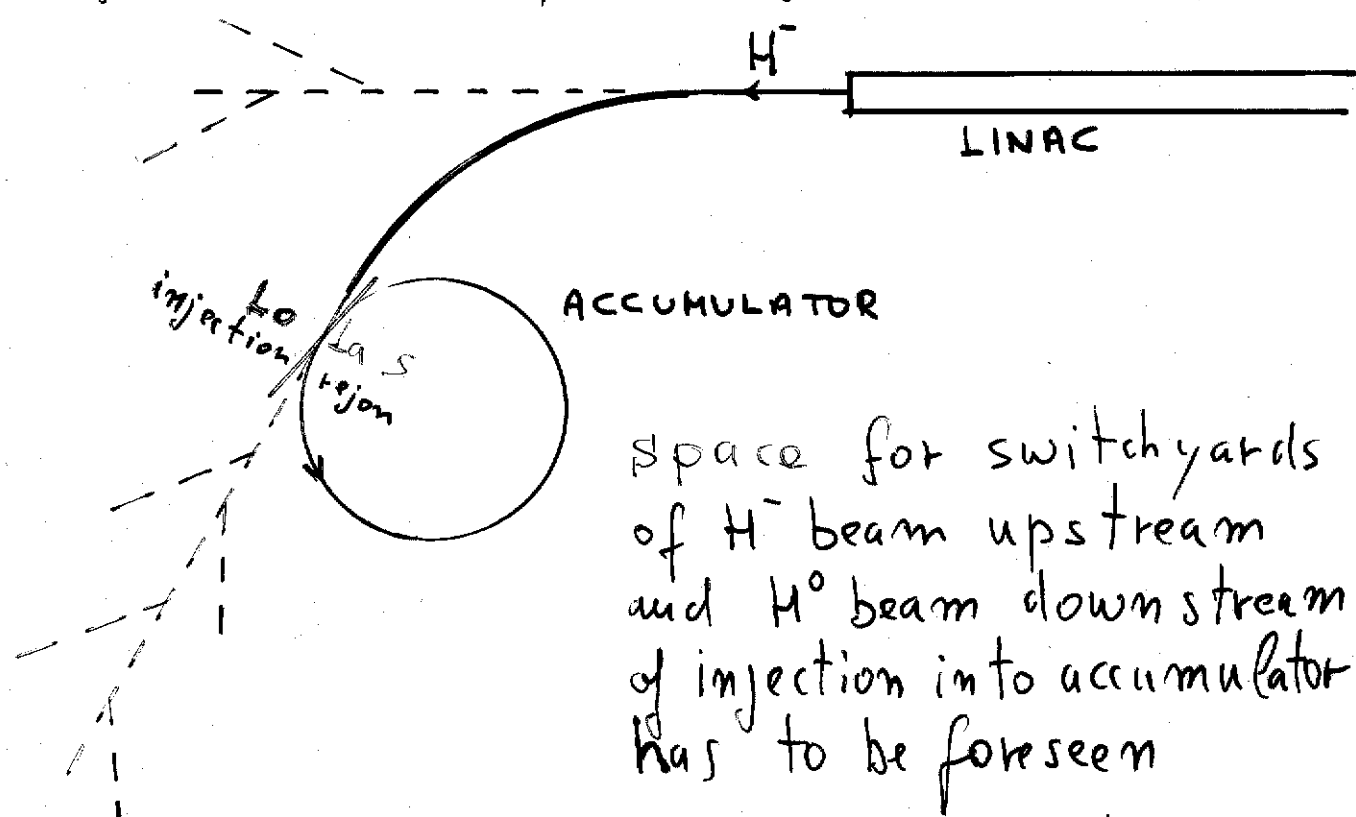
LoLAS INTEGRATION into p⁺ accumulator

- need $L \sim 1\text{m}$ interaction region H°-Light
- need $\sim 10\text{m}$ long optical bench to have FP mirrors 10 cm apart from H° beam
- choose γ and α so that $\frac{1}{\hbar}(1-n^2)R\gamma = v_{FP} \gamma(1+\beta \cos\alpha)$
- feedback onto linac to keep $\langle p \rangle$ stable to possibly 10^{-4}
- feedback onto wigglet trim coil to compensate variation of $\langle p \rangle$ by overall shift of energy of Stark state of $|n, 0, m-1, 0\rangle$ level
- install 2nd FP for redundancy-safety (cannot double H° stripping ...)
- H° beam optics is controlled outside p⁺ accumulator by H⁻ beam steering and H⁻ Lorentz stripping magnet. For $n \geq 4$ p⁺ angular dispersion due to Lorentz stripping in wigglet pole can be less than H° beam one
- H°($n \geq 4$) Lorentz stripping easy. (choice of wigglet pole B field characteristics (slope, max field) to be done to optimize painting.)

- $H^0(n \geq 4)$ Lorentz stripping following laser excitation to $n \geq 4$ in wigglet valley and $H^0(n \geq 4)$ Lorentz stripping simultaneous to Laser excitation to $n \geq 4$ Stark sublevel Stark broadened in peak field region of wigglet
 - require same length L of H^- Light overlap-interaction region given same light power density
- excitation in valley gives more flexibility for painting (and less p^+ angular dispersion if required)
- excitation in peaks to $n \geq 4$, results in total stripping of generated $H^0(n)$.
- excitation of H^- to $H^-(F)$ might in future permit to adapt LOLAS injection to cases where H^0 injection into p^+ accumulator would not have been foreseen. Foil to be substituted by interaction region with light needs not to be in a magnet to minimize changes, since F H^- state broadens, splits, then disappears due to L_z Stark field.

• CONCLUSIONS + comments

- ALL PHYSICAL INGREDIENTS of LOLAS injection experimentally assessed
- CRITICAL ITEM is Power Density in FP
 I_{FP}
- SCHEME FORESEES and IMPLIES from the beginning operation in parallel of high and low duty cycle users of the injector linac



- FP cavity photon losses due to absorption by stripped H^0 's recovered between linac pulses
- accumulation can be interrupted simply by tuning of trim coil of injection wiggler to drive \mathcal{N} out of resonance
- very little bending power needed to bring H^- directly to downstream switchyard during maintenance in I.F.